Field Evaluation of Wisconsin Modified Binder Selection Guidelines - Phase II

Hussain Bahia, Ph.D.
Hassan A. Tabatabaee, Ph.D.
Tirupan Mandal

University of Wisconsin Madison

Ahmed Faheem, Ph.D.

University of Wisconsin Platteville
Bloom Companies, LLC

WisDOT ID no. 0092-13-02

December 2013

RESEARCH & LIBRARY UNIT

WISCONSIN HIGHWAY RESEARCH PROGRAM

WISCONSIN DOT

PUTTING RESEARCH TO WORK

Field Evaluation of Wisconsin Modified Binder Selection Guidelines - Phase II

Wisconsin Highway Research Program Project: 0092-13-02

Final Report

By:

Hussain Bahia, Ph.D.

Hassan A. Tabatabaee, Ph.D.

Tirupan Mandal

University of Wisconsin Madison

Ahmed Faheem, Ph.D.

University of Wisconsin Platteville

Bloom Companies, LLC

University of Wisconsin Madison

Modified Asphalt Research Center

December 2013

DISCLAIMER

This research was funded through the Wisconsin Highway Research Program by the Wisconsin Department of Transportation and the Federal Highway Administration under Project 0092-13-02. The contents of this report reflect the views of the authors who are responsible for the facts and accuracy of the data presented herein. The contents do not necessarily reflect the official views of the Wisconsin Department of Transportation or the Federal Highway Administration at the time of publication.

This document is disseminated under the sponsorship of the Department of Transportation in the interest of information exchange. The United States Government assumes no liability for its contents or use thereof. This report does not constitute a standard, specification or regulation.

The United States Government does not endorse products or manufacturers. Trade and manufacturers' names appear in this report only because they are considered essential to the object of the document.

Technical Report Documentation Page

1. Report No. WHRP	2. Government Accession No	3. Recipient's Catalog No
4. Title and Subtitle Field Validation of Wisconsin Modified Binder Selection Guidelines – Phase II		5. Report Date December 2013 6. Performing Organization Code
7. Authors Hussain U. Bahia, Hassan A. Tabatabaee, Tirupan Mandal, Ahmed Faheem		8. Performing Organization Report No.
9. Performing Organization Name and Address University of Wisconsin-Madison Civil and Environmental Engineering Department 1415 Engineering Drive, Madison, WI 53705		10. Work Unit No. (TRAIS) 11. Contract or Grant No. WisDOT SPR# 0092-13-02
12. Sponsoring Agency Name and Address Wisconsin Department of Transportation Division of Business Management Research & Library Unit 4802 Sheboygan Ave. Rm 104 Madison, WI 53707		13. Type of Report and Period Covered Final Report, 9/2012 - 12/2013 14. Sponsoring Agency Code
15. Supplementary Notes		

16. Abstract

The purpose of this project was to continue phase I of the study with the objective of identifying promising procedures and applicable modified binder specification criteria for use in Wisconsin, based on comparison of test results to field performance. Field performance was assessed through condition surveys conducted between 2004 and 2012 as part of both phase I and phase II of the project.

The Linear Amplitude Sweep test, standardized under AASHTO TP101, was considered and evaluated as a potential test. The test related very well to field performance when performed at the required Superpave intermediate temperature grade of the project location, and the fatigue life parameter, Nf, was determined at the peak stress. A set of preliminary performance criteria were proposed based on the target mix design type and target traffic grade.

The Single Edged notched Bending procedure (BBR-SENB), based on the modification of the Bending Beam Rheometer test, currently under consideration by AASHTO for provisional standardization, was used to assess resistance to thermal cracking. The BBR-SENB results correlated well with the observed field thermal cracking when tests were conducted at the project location low temperature PG specification temperature. A specification and preliminary performance criteria is developed and suggested for use of the BBR-SENB as a binder selection and characterization test.

In terms of rutting resistance it was shown that the studied Wisconsin binders exceeded the most extreme binder rutting grade requirements according to AASHTO MP 19 (MSCR) at the local high performance temperatures. The binder test results were unable to accurately relate to the observed field conditions. It was shown that the aggregate structural properties could capture a trend that better reflected that of the field rutting behavior. Results indicate that proper ranking of material in terms of rutting resistance is not possible without consideration of both binder properties and aggregate structure, as both factors contribute significantly to the pavement rutting performance.

17. Key Words	18. Distribution Statement
Modified binder characterization, field performance, Linear Amplitude Sweep, Single Edged notched Bending, Multiple Stress Creep and Recovery, Image Analysis, Mastic viscosity	No restriction. This document is available to the public through the National Technical Information Service 5285 Port Royal Road Springfield VA 22161

18. Security Classif.(of this report)	19. Security Classif. (of this page)	20. No. of Pages	21. Price
Unclassified	Unclassified	89	

Form DOT F 1700.7 (8-72) Reproduction of completed page authorized

EXECUTIVE SUMMARY

The purpose of this project was to continue phase I of the study with the objective of identifying promising procedures and applicable modified binder specification criteria for use in Wisconsin, based on comparison of test results to field performance. Field performance was assessed through condition surveys conducted between 2004 and 2012 as part of both phase I and phase II of the project.

The Linear Amplitude Sweep test, standardized under AASHTO TP101, was considered and evaluated as a potential test. Two failure criteria were evaluated for calculation of the "A" parameter in the LAS fatigue power law. The best correlations with field performance were found when testing at the required Superpave intermediate temperature grade of the project location and calculating the Nf value corresponding to the damage level at the peak stress. A set of preliminary performance criteria were proposed based on the target mix design type and target traffic grade.

The Single Edged notched Bending procedure (BBR-SENB), based on the modification of the Bending Beam Rheometer test, currently under consideration by AASHTO for provisional standardization, was used to assess resistance to thermal cracking. The BBR-SENB results correlated well with the observed field thermal cracking when tests were conducted at the project location low temperature PG specification temperature. A procedure was introduced for thermal cracking evaluation of modified binders using the BBR-SENB test at the project location low temperature PG specification temperature (average annual minimum pavement temperature + 10°C) and a preliminary failure limit and acceptance criterion was defined for qualifying binder results in terms of thermal cracking resistance using RTFO aged binders and estimated for PAV-

aged conditions. Based on the current data it is recommended that PAV-aged conditions be used for a more conservative controlling of binder failure properties.

In terms of rutting resistance it was shown that the studied Wisconsin binders exceeded the most extreme binder rutting grade requirements according to AASHTO MP 19 (MSCR) at the local high performance temperatures. The binder test results were unable to accurately relate to the observed field conditions. Information reported with regards to construction conditions and resultant variation in field short-term aging compared to that achieved using the RTFO were noted as possible contributing factors to the lack of relationship. Nonetheless, it was shown that the aggregate structural properties measured using simple image analysis procedures could capture a trend that better reflected that of the field rutting behavior. Results indicate that proper ranking of material in terms of rutting resistance may not be possible without consideration of both binder properties and aggregate structure, as both factors contribute significantly to the pavement rutting performance.

AKNOWLEDGEMENTS

This study was sponsored by the Wisconsin Highway Research Program. The continuous support of WisDOT and WHRP is greatly appreciated, with specials thanks to Ms. Judie Ryan and the Flexible Pavement Technical Oversight Committee.

The authors also gratefully acknowledge the cooperation of the following UW students, Ms. Raquel Moraes and Mr. Nima Roohi, who contributed to the laboratory testing and analysis. Their help is greatly appreciated.

TABLE OF CONTENTS

DISCLAIMER iii
EXECUTIVE SUMMARY v
AKNOWLEDGEMENTS vii
LIST OF FIGURES 10
LIST OF TABLES 12
CHAPTER ONE: INTRODUCTION 13
Introduction 13
Project Background 14
Research Approach and Report Structure 14
Field Distress Survey 15
CHAPTER TWO: FATIGUE CRACKING RESISTANCE 18
Background 18
Selected Projects 22
Binder Testing 23
Performance Data 30
Proposed Procedure for Fatigue Evaluation (LAS) 40
Summary and Conclusions for Binder Fatigue Evaluation 41
CHAPTER THREE: RESISTANCE TO THERMAL CRACKING 44
Background 44
Selected Projects 46
Binder Testing 47
Performance Data 50
Proposed Procedure for Thermal Cracking Evaluation (BBR-SENB) 58
BBR-SENB Apparatus and Device Requirements 58
Summary and Conclusions for Thermal Cracking Evaluation of Binders 60
CHAPTER FOUR: RUTTING RESISTANCE 62
Background 62
Selected Projects 65

Binder Testing 66
Characterization of internal aggregate structure by means of Digital Imaging Analysis 72
Performance Data 77
Summary and Conclusions for Evaluation of Rutting Resistance 80
CHAPTER FIVE: CONCLUSIONS AND RECOMMENDATIONS 82
Fatigue Characterization 82
Low Temperature Characterization 83
Rutting Characterization 85
REFERENCES 86

LIST OF FIGURES

Figure 1. Ability of standard and research-grade rheometers in terms of achieving (a) target apparent strain, and (b) apparent stress response using the continuous strain sweep.....19
Figure 2. Linear Amplitude Sweep Fatigue Power Law Corefficitents ("A" and "B") using both failure criteria from tests performed at 15°C. 25
Figure 3. LAS Nf results using both failure criteria at 15°C for (a) 2.5% strain, and (b) 5% strain. 26
Figure 4. Linear Amplitude Sweep Fatigue Power Law Corefficitents ("A" and "B") using both failure criteria from tests performed at IT PG specification temeprature. 28
Figure 5. LAS N_f results using both failure criteria for (a) 2.5% strain, and (b) 5% strain at IT PG specification temperature. 29
Figure 6. Relationship between field performance and the $|G^*|\sin\delta$ 32
Figure 7. Relationship between field performance in terms of percent cracked segments per field section and LAS parameters from tests at 15°C 33
Figure 8. Relationship between field performance in terms of percent cracked segments per field section and LAS parameters from tests at IT PG temperature 34
Figure 9. Estimation of number of ESALs to a fixed damage level in all sections 35
Figure 10. Relationship between field performance and LAS parameters by comparing to the number of ESALs in the field to a fixed damage level.....37
Figure 11. Comparison between LAS results at two strain levels at RTFO and PAV aged conditions (solid trend line shows trend after removal of large data value) 38
Figure 12. Lack of correlation shows that N_f at peak stress should not be assumed equivalent to the strain at peak stress 41
Figure 13 (a) BBR-SENB sample mold and dimensions, and (b) BBR-SENB loading device and setup. 46
Figure 14. BBR-SENB results from on selected field section binders at -18°C 49
Figure 15. Comparison of trend between BBR-SENB results and BBR T_c temperatures.....50
Figure 16. Comparison of BBR-SENB failure parameters with field section thermal cracking PCI (larger deduct value = higher quantity and/or severity of thermal cracking) 52
Figure 17. Comparison of BBR-SENB failure parameters with field section thermal cracking PCI at the exact LTPG temperature (larger deduct value = higher quantity and/or severity of thermal cracking) 53
Figure 18. BBR-SENB proposed preliminary specification graph at RTFO-aged conditions (lower left triangle fails the specification) 55
Figure 19. Comparison between BBR-SENB results at RTFO-aged and PAV-aged conditions for (a) failure deflection, and (b) failure energy. 56
Figure 20. Example of estimated BBR-SENB specification graph at PAV-aged conditions (lower left triangle fails the specification) 57
Figure 21. Modified mold assembly for preparation of BBR-SENB beams. 59

Figure 22. Loading device in BBR-SENB 59
Figure 23. Beam supports to ensure notch alignment.....59
Figure 24. Standard MSCR Results for binders at the local climate PG (dashed line shows AASHTO MP 19 limit for the "S" grade, dotted line shows the "E" grade limit).....67
Figure 25. Superpave rutting test results at multiple temperatures (dashed line is RTFO grade criteria) 68
Figure 26. MSCR Results for MnROAD binders at 58°C (dashed line shows AASHTO MP 19 limit for the "S" grade, dotted line shows the "E" grade limit) 69
Figure 27. Comparison of binder measures ($G^*/\sin\delta$ and J_{nr}) and the observed field rut depth...71
Figure 28. Illustration. Definition of the aggregate proximity line 74
Figure 29. Illustration. Schematic of contact orientation calculation 74
Figure 30. Illustration. Contact lines and orientation in real mixtures. (Normal to contacts lines are shown with arrows).....76
Figure 31. Illustration. Aggregate skeleton- connectivity (lines represent stress paths) 76
Figure 32. Gradation of MnROAD test sections.....77
Figure 33. Filtered images of aggregate structure for (a) C-77, (b) C-22, and (c) C-20.....78
Figure 34. Comparison of TPL and field performance (rut depth) 79

LIST OF TABLES

Table 1 List of Projects Examined in the Study....16
Table 2. Information corresponding to selected field section for fatigue test evaluation....22
Table 3. Required Passing Grade Temperature from LTPPBind v3.1....23
Table 4. Results of Linear Amplitude Sweep tests performed at 15°C for $N_{f35\%}$....24
Table 5. Results of Linear Amplitude Sweep tests performed at 15°C for N_{fPeak}....24
Table 6. Results of Linear Amplitude Sweep tests performed at IT PG specification temperature for $N_{f35\%}$....27
Table 7. Results of Linear Amplitude Sweep tests performed at IT PG specification temperature for N_{fPeak}....28
Table 8. Field performance based on observation of longitudinal cracking....31
Table 9. LAS criteria evaluated against field performance tested at 15°C and the IT PG....31
Table 10. Number of ESALs corresponding to 75% of segments in section showing fatigue damage....36
Table 11. Suggested preliminary LAS minimum N_f limits for pavement design based on mixture category and AASHTO MP-19 grade....37
Table 12. Estimated LAS minimum limits at PAV conditions used to demonstrate expected potential for dervinig such limits based on PAV-aged LAS tests....39
Table 13. Information corresponding to selected field section for thermal cracking binder evaluation....47
Table 14. Summary of critical temperature values derived from phase I tests....48
Table 15 List of projects showing thermal related cracking, corresponding deduct values from ASTM D6433, binder grade, and average annual low temperature....51
Table 16. List of Pooled Fund and LTPP binders used for preliminary criteria development (Bahia, et al., 2012; Marasteanu, et al., 2012)....54
Table 17. Selected MnROAD cells and binder modification properties....66
Table 18. Field sections tested at corresponding design ESALs and speed....66
Table 19. Rutting Performance of MnROAD cells after 30 months of loading....70
Table 20. Regression analysis results for binder and aggregate rutting paramters against a rut depth response....80

CHAPTER ONE: INTRODUCTION

Introduction

Current Superpave binder specifications, as used in Wisconsin and many other states, are based on linear viscoelastic properties. Furthermore, the current specifications were primarily developed for unmodified binders. However, research has demonstrated the importance of damage resistance characterization of asphalt binders with respect to pavement distresses (Bahia, et al., 2001). Unmodified and modified binders often perform comparably within the linear viscoelastic range. However, modified binders often demonstrate superior damage resistance. A number of procedure have been introduced in recent years to address the need for damage characterization test procedures for proper assessment and selection of modified binders, examples of which are the linear amplitude sweep (LAS) test (Johnson 2010, Hintz et al. 2011), the dynamic shear rheometer elastic recovery (ER-DSR) (Clopotel & Bahia, 2012), Single Edged Notched Bending (BBR-SENB) test (Velasquez, et al., 2011), and a modified method for conduction of the multiple stress creep and recovery (MSCR) test (Bahia, et al., 2011). Furthermore, recent findings suggest that determination of compaction temperatures or assessment of resistance to rutting solely based binder parameters and properties is insufficient, as the aggregate structure and the complex interaction between binder and aggregate structural properties can have detrimental effects on rutting resistance and compactability of mixtures (Roohi, et al., 2012; 2013). Thus investigation of potential method incorporating an understanding of aggregate structure and interaction of binder and aggregate is of essential importance for assessment of such behavior.

Project Background

In October 2007 the Wisconsin Department of Transportation (WisDOT) and the Wisconsin Highway Research Program completed, "SPR 0092-03-13: Field Validation of Modified Binder Selection Guidelines." The study served as an initial step towards validating WisDOT's asphalt binder selection criteria. Field sites were identified, and HMA materials (asphalt binder and loose mix) were sampled. The most valuable product of this research was the characterization of the as-built asphalt binder material properties using newly-developed test methods that focused on damage-resistance characteristics. Early-life pavement distress surveys were conducted to evaluate the ability of these test methods to quantify the effect of use of modified binders on field performance; however, there was difficulty in differentiating the performance of the pavements due to the relatively short time frame over which they were in service.

Thus it was concluded that the potential exists that application of new characterization techniques in conjunction with field performance data from the existing test sections will improve WisDOT's understanding of the critical asphalt binder properties that influence field performance. The present study and report is an effort to address these needs and provide further insight into potential procedures for evaluating and selecting modified binders using performance based criteria.

Research Approach and Report Structure

In the present study a set of modified binders corresponding to constructed field section across Wisconsin were tested using recently developed characterization procedures under consideration or standardized by AASHTO as provisional standards. The purpose of the project was to identify promising procedures and applicable modified binder specification criteria for use in Wisconsin,

based on comparison of test results to field performance. Field performance was assessed through condition surveys conducted between 2004 and 2012 as part of both phase I and phase II of the project.

The performance of the surveyed field sections was evaluated in three main categories based on temperature range of the interest (i.e. high, intermediate, and low service temperatures). These temperature ranges correspond to rutting, fatigue damage and thermal cracking distress in the pavement. Results of binder testing and analysis, along with comparative studies to measured field performance are conducted in a separate chapter for each of the aforementioned temperature ranges and distress modes. Based on the results suggestions are mode for consideration as modifications to the current WisDOT binder selection criteria and specification.

Field Distress Survey

The field inspection component of this study involved the inspection of 12 sites identified in the first round, as shown in Table 1. The inspection process followed the ASTM D6433 standard procedure. In this procedure, random subsections are identified for the site at hand. An inspection of the standard distresses is then conducted, highlighting the extent of each distress (value) and the severity. According to the information collected, the ASTM procedure demonstrates means for calculating a "deduct" value that is representative of the level of damage due to a specific distress. After all the deduct values for all the available distresses are determined, the Pavement Condition Index (PCI) is determined.

Table 1 List of Projects Examined in the Study

Project ID	Project	Location (County)	Year of Construction	Mixture Type	Project Title
1080-00-72	USH 12	WALWORTH	2003	E-1	WHITEWATER BYPASS (USH 12)
1170-13-70	USH 51	IRON	2004	E-3	STH 77-USH 2- City of Hurley USH 51
9040-09-70	STH 17	ONEIDA/VILAS	2003	E-3	POLLYANNA LN-STH 70-STH 17
9140-07-70	STH 64	LANGLADE	2003	E-3	CHARLOTTE COURT-CLOVER ROAD (STH 64)
7132-04-61	STH 93	BUFFALO & TREMPEALEAU	2004	E-1	STH 93 & STH 95
5300-04-74	USH 12	DANE	2005	E-10	WEST MADISON BELTLINE (GAMMON RD-WHITNEY WAY)
7200-05-70	STH 35	ST. CROIX	2005	E-10	RIVER FALLS-HUDSON ROAD (HANLEY ROAD INTERCHANGE)
4657-11-71	CTH A	OUTAGAMIE	2005	E-10	LYNNDALE DRIVE (CTH A)
6590-00-70	STH 110	WAUPACA	2003	E-1	PINE, MAIN & MILL STREETS-CITY OF WEYAUWEGA (STH 110)
1130-12-71	USH 41	BROWN	2003	E-30	DE PERE-GREEN BAY - LOMBARDI AVE- IH 43 (USH 41)
3120-06-70	STH 67	WALWORTH	2003	E-1	STH67-WALWORTH COUNTY
4100-10-71	USH 151	MANITOWOC	2003	E-10	CALUMET AVE., MANITOWOC (SOUTH 41st STREET-26th STREET)

In calculation of the PCI, distresses are recorded based on their severity, based on which the deduct value corresponding to each severity level is calculated. The deduct values represent the combined values for a given distress type. This deduct value is used in the data analysis as a measure of the impact the different distress types on the overall pavement condition.

The 2012 field distress survey was conducted on randomly selected 200ft sections within each site. The randomization was conducted prior to visiting each site to eliminate bias in the selection of the inspection sections. After the random selection of the test section, the entire length of the pavement section was driven to assure the uniformity of the roadway and that the selected section does not represent a special or unique segment of the roadway.

The information on the distress level collected in this study provides the means necessary to quantify the impact of each distress on the overall pavement condition, while provide a mechanism to compare the distress level to that obtained from the previous phase of this study. It is important to note that a number of the sites, including 9040-09-70 and 1130-12-71 in Vilas and Brown counties respectively, had been resurfaced and repaved before the 2012 survey was conducted. Therefore, for these sites no distress survey was conducted. Distress data from the previous phase of this study was converted to deduct values using the distress description and attributes provided. This allows for examining the deterioration in pavement condition over time.

In relation to this study, thermal cracking and wheel path (WP) longitudinal cracking are the most critical. While alligator cracking is evident in two of the projects, no such type of cracking was observed in the previous phase. In addition, no rutting deformation was observed in all the random sections studied for this project. Pavement surface quality appeared to be greatly impacted as demonstrated by the consistent presence of raveling and polished aggregate surface for most of the projects surveyed. This is most likely due to the plowing of snow during winter.

CHAPTER TWO: FATIGUE CRACKING RESISTANCE

Background

In phase I of this study, field performance was related to the Np20 parameter, derived from the time sweep test first proposed by Bahia et al. (2001). To derive the fatigue life relationship for a specific binder and temperature the time sweep test was performed at multiple input energy levels. These energy levels are related to the overall strain and loading level in the pavement layer, and thus could be related to highway classification or pavement structure. Further details on the procedure and specification can be found in the literature (Nam, et al., 2005; Delgadillo & Bahia, 2005).

Although the test results showed promising trends with the field performance in phase I, since then the time sweep test method has been replaced by other newer procedures, despite the promising relation to performance. The main reason for this has been challenges with regards to repeatability of the time sweep test as well as the practicality of performing the lengthy time sweep procedures, in some cases lasting for hours.

The Linear Amplitude Sweep (LAS) test is the primary method under investigation as an accelerated fatigue procedure (Hintz, 2012; Johnson & Bahia, 2010). The test is performed using the DSR 8-mm parallel plate geometry in strain-controlled mode at the same temperature and loading frequency as the time sweep, but the load amplitude is systematically increased to accelerate damage in the specimen. Use of viscoelastic continuum damage mechanics allows for prediction of fatigue life at any strain amplitude from a single 30 minute test, thus allowing for consideration of pavement structure (i.e., strain) and traffic (i.e., number of cycles to failure). The procedure has been validated through comparison with field performance of Long-Term

Pavement Performance (LTPP) test sections (Hintz, et al., 2011). The procedure received the FHWA Binder ETG's approval in 2011 and designated a provisional AASHTO standard procedure under AASHTO TP101 in 2012.

An initial 100 cycles is applied at 0.1% strain to determine undamaged linear viscoelastic properties. The procedure consists of ramping strain amplitude, beginning at 0.1% and ending at 30% applied strain, over 3100 cycles of loading at 10 Hz. A graphical example of this loading scheme is shown in Figure 1(a). Through communications with major Rheometer manufacturers and user experience it was determined that all current standard rheometers have the capability of performing strain sweeps in which strain is increased at a rate of 0.1% per second at a high precision without difficulty (Figure 1(b)).

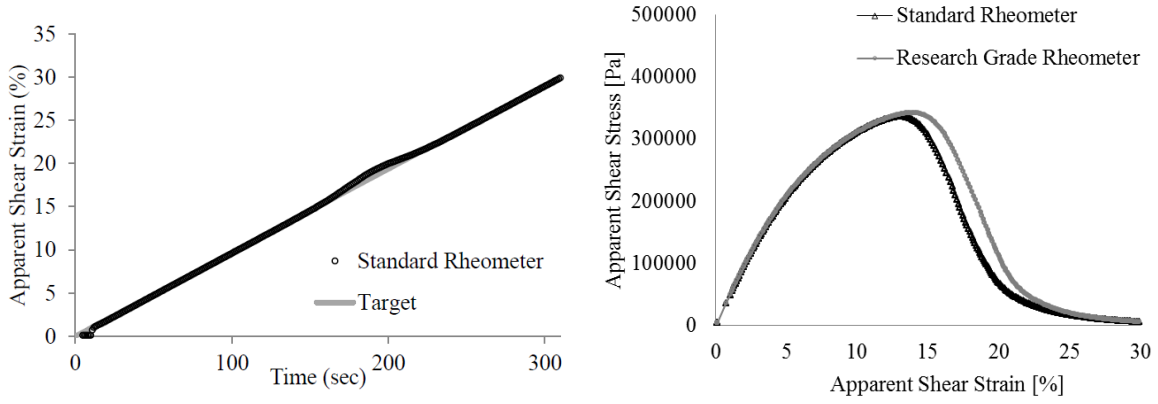

(a) **(b)**

Figure 1. Ability of standard and research-grade rheometers in terms of achieving (a) target apparent strain, and (b) apparent stress response using the continuous strain sweep

Once the strain sweep is applied to the sample, the damage accumulation for the LAS test can be determined through VECD analysis, resulting in the fatigue power law damage model (equation 1), and the corresponding coefficients, *A* and *B*.

$$N_f = A\ (\gamma_{max})^{-B} \qquad (1)$$

Nf is the number of cycles to fatigue failure, which is the traffic volume failure criteria, γ_{max} is the maximum tensile strain expected in the binder phase under traffic loading, which will be a function of pavement structure. Currently the strain values of 2.5 and 5% strain are used to calculate the LAS fatigue life. The binder strain is assumed to be by average 50 times larger than that of the bulk mixture strain, based on earlier research (Kose, et al., 2000).

The *A* coefficient is determined through VECD analysis of the continuous oscillatory amplitude sweep. To determine the undamaged rheological behavior for input into the VECD calculations a frequency sweep test is needed. The procedure consists of applying constant low-level load amplitude (0.1% strain) to avoid damaging the specimen over a range of loading frequencies (typically from 0.1 to 30 Hz, depending on equipment capabilities). The logarithmic slope of the storage modulus ($G'(\omega)$) as a function of angular frequency (*m*) is used to calculate the damage accumulation and the parameter *B*, as shown in equations 2 and (3).

$$D(t) \cong \sum_{i=1}^{N} [\pi \gamma_0^2 (C_{i-1} - C_i)]^{\frac{\alpha}{1+\alpha}} (t_i - t_{i-1})^{\frac{1}{1+\alpha}} \qquad (2)$$

$$B = 2\alpha \qquad (3)$$

where:

- $C(t) = \frac{|G^*| sin\delta(t)}{|G^*| sin\delta_{initial}}$ which is |G*|sinδ at time *t* divided by the initial "undamaged" value of |G*|sinδ.
- γ_0 = applied strain for a given data point, percent
- |G*| = Complex shear modulus, MPa

$\alpha = 1/m$

- t = testing time, seconds

By linearization of the log of the damage accumulation (log(D(t)) versus time, the resulting coefficients can be used to calculate the fatigue law A parameter as shown in equation 4 to 6.

$$\log(C_0 - C(t)) = \log(C_1) + C_2 \cdot \log(D(t)) \quad (4)$$

$$A = \frac{f\left(D_f\right)^{\kappa}}{k(\pi I_D C_1 C_2)^{\alpha}} \quad (5)$$

$$D_f = \left(\frac{C_f}{C_1}\right)^{1/C_2} \quad (6)$$

where:

- C_0 = 1, the initial value of C,
- C_1 and C_2 = curve-fit coefficients,
- f = loading frequency (10 Hz).
- k = 1 + (1 – C_2) α
- D_f = damage level failure criteria
- C_f = normalized modulus at failure criteria

The damage level failure criteria should be defined in a manner that most closely reflects failure behavior in the field. In the present study two criteria were investigated:

1. C_f is defined as C(t) corresponding to 35% reduction in initial |G*|sinδ, in which C(t) is the ratio of the |G*(t)|sinδ(t) to its initial value ($|G^*_0|\sin\delta_0$).
2. C_f is defined as C(t) corresponding to the peak shear stress experienced during the test, in which C(t) is the ratio of the |G*(t)| to its initial value ($|G^*_0|$).

The second criterion was inspired by a recent study on relation of the LAS procedure to mixture fatigue testing (Safaei, et al., 2013). Comparison of results to field performance will be used as the basis of selecting one of the proposed failure criteria for use in evaluation of modified binders in Wisconsin. Further information on the LAS procedure and development can be found in the literature (Hintz, et al., 2011; Hintz, 2012).

Selected Projects

For the field evaluation of the fatigue characterization parameters, section corresponding to the modified binders used in phase I were used for comparison with previous results. The modified binders were graded PG58-34, PG64-28, and PG70-28. All projects were constructed in 2003 with a design life of 20 years. For each section the traffic information was previously derived from the design documents. The field section and binder information is shown in Table 2.

Table 2. Information corresponding to selected field section for fatigue test evaluation

Project Name	DOT Project ID	Binder	Design ESALs	Traffic Growth Rate
STH 17 Rhinelander Bypass	9040-09-70	58-34	2029400	2.4%
Charlotte Court - Clover Road (STH 64)	9140-07-70	58-34	1511101	1.5%
South County Line - CTH M (USH 51)	1177-10-70	58-34	1898000	1.5%
Pine, Main & Mill Streets City of Weyauwega (STH 110)	6590-00-70	64-28	861000	2.0%
De Pere-Green Bay-Lombardi Ave - IH 43 (USH 41)	1130-12-71	64-28	19388800	2.1%
STH67 – Walworth County	3120-06-70	64-28	> 1000000*	1.7%
Airport Freeway (IH 894)	1090-14-70	70-28	15972400	1.6%

*As design data was unavailable for this section, the mixture design rating (E-1) was used as basis of traffic level.

Binder Testing

Binder testing was performed using the Linear Amplitude Sweep on RTFO aged binders. The tests were performed at two temperature regimes. The first set of tests was all performed at 15°C. This temperature was chosen in phase I as the yearly average pavement temperature in Wisconsin and was used for binder fatigue testing using the Np20 procedure in Phase I of the project.

The second set of tests was performed at the local intermediate performance grade specification temperature as determined in AASHTO M320. The reason for using this temperature criterion was to use test conditions better representing local conditions for each binder. For determination of the testing temperatures to be considered, the LTPPBind v3.1 software was used to determine the average condition in the county in which the highway section was located at a reliability level of 98%. The results are shown in Table 3.

Table 3. Required Passing Grade Temperature from LTPPBind v3.1

Project Name	WI County	DOT Project ID	Binder	IT PG Specification
STH 17 Rhinelander Bypass	Oneida-Vilas	9040-09-70	58-34	13°C
Charlotte Court - Clover Road (STH 64)	Langlade	9140-07-70	58-34	16°C
South County Line - CTH M (USH 51)	Marquette	1177-10-70	58-34	16°C
Pine, Main & Mill Streets City of Weyauwega (STH 110)	Waupaca	6590-00-70	64-28	16°C
De Pere-Green Bay-Lombardi Ave - IH 43 (USH 41)	Brown	1130-12-71	64-28	16°C
STH67 – Walworth County	Walworth	3120-06-70	64-28	19°C
Airport Freeway (IH 894)	Milwaukee	1090-14-70	70-28	19°C

Using the analysis procedure described in the previous sections, the LAS results were calculated as shown in Table 4 and Table 5, Figure 2, and Figure 3 for tests at 15°C. Two failure criterions were used for analysis.

Table 4. Results of Linear Amplitude Sweep tests performed at 15°C for $N_{f35\%}$

Binder Name	A	COV	B	COV	Nf 2.5%	COV	Nf 5%	COV
1090-14-70	103090	5.9%	-3.47	0.5%	4283	4.2%	386	2.9%
9040-09-70	350401	3.1%	-3.34	0.1%	16396	3.4%	1617	3.6%
1130-12-71	129599	4.8%	-3.07	0.0%	7763	4.9%	923	4.9%
1177-10-70	234773	3.7%	-3.00	0.3%	15011	2.9%	1875	2.3%
6590-00-10	152202	1.8%	-3.21	0.3%	8070	2.6%	875	3.2%
3120-06-70	284455	8.5%	-3.65	0.1%	10003	8.2%	795	7.9%
9140-07-70	261187	11.9%	-3.06	1.1%	15746	8.8%	1882	6.4%

Table 5. Results of Linear Amplitude Sweep tests performed at 15°C for N_{fPeak}

Binder Name	A	COV	B	COV	Nf 2.5%	COV	Nf 5%	COV
1090-14-70	262288	3.2%	-3.47	0.5%	10906	4.9%	984	6.2%
9040-09-70	303830	2.2%	-3.34	0.1%	14216	1.9%	1402	1.7%
1130-12-71	143563	6.3%	-3.07	0.0%	8599	6.2%	1022	6.1%
1177-10-70	247962	2.0%	-3.00	0.3%	15856	1.2%	1981	0.6%
6590-00-10	162265	6.6%	-3.21	0.3%	8601	5.8%	932	5.2%
3120-06-70	361598	15.6%	-3.65	0.1%	12714	15.2%	1010	15.0%
9140-07-70	273749	17.6%	-3.06	1.1%	16488	14.5%	1969	12.1%

In Table 4 failure is determined based on 35% reduction in $|G^*|\sin\delta$, while the results in Table 5 were calculated at the damage level corresponding to the peak stress response. A

relatively high spread in the results of the different binders is observed, which is desirable for a characterization and selection parameter. Furthermore, the coefficients of variation for all tests are generally less that 10%, which is considered very good for a damage test.

Figure 2 shows that difference in two criteria is simply on the interpretation of the "A", the damage parameter, with "B", the rheological parameter remaining unchanged. For many binders both failure criteria yield relatively similar results, with main difference being for binder 1090-14-17, which showed the weakest response using the 35% reduction criteria, while showing a relatively average performance if the peak stress criteria is utilized, as can be seen clearly in Figure 2 and Figure 3.

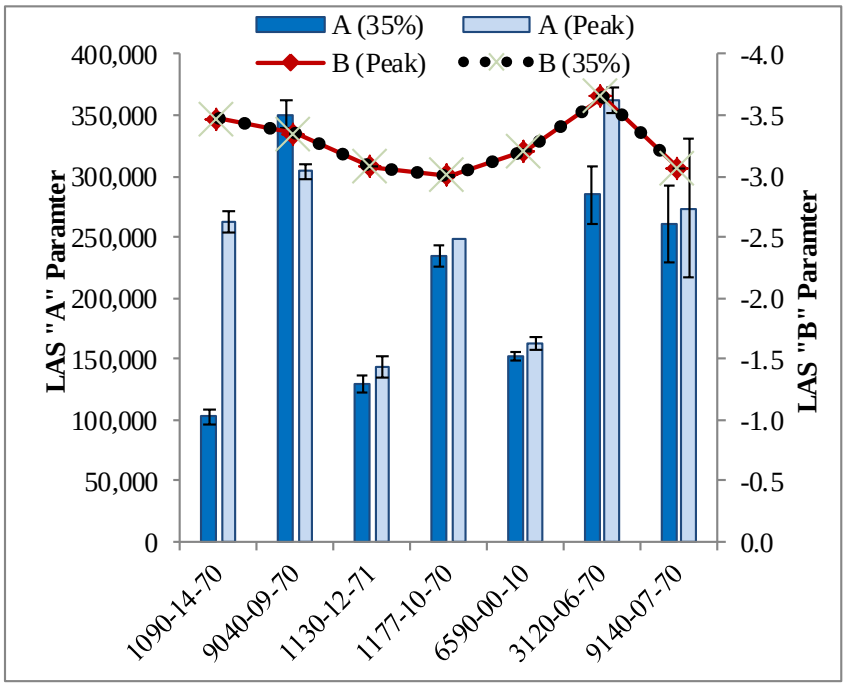

Figure 2. Linear Amplitude Sweep Fatigue Power Law Corefficitents ("A" and "B") using both failure criteria from tests performed at 15°C.

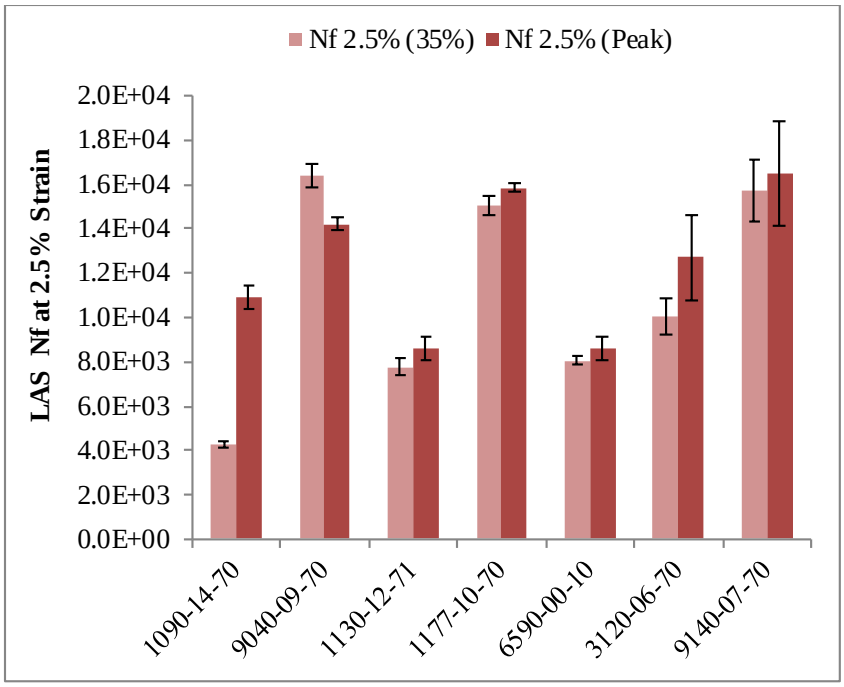

(a)

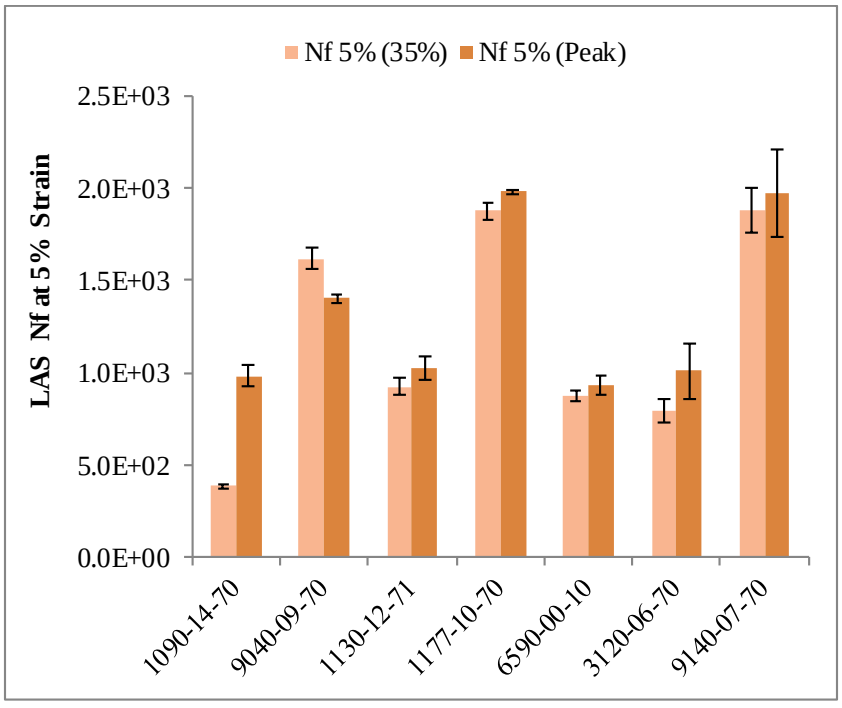

(b)

Figure 3. LAS Nf results using both failure criteria at 15°C for (a) 2.5% strain, and (b) 5% strain.

Table 6 and Table 7 show the analysis results from LAS tests performed at the intermediate performance grade specification temperature. As in the analysis at 15°C, two failure criterions were used for the analysis of the tests performed at the PG intermediate specification temperature, with failure in Table 6 being determined based on 35% reduction in $|G^*|\sin\delta$, and the results in Table 7 being calculated at the damage level corresponding to the peak stress response. What is noteworthy in results at both 15°C and the IT PG temperature is that the peak stress N_f criterion results in a smaller spread in the results compared to the 35% reduction criteria. This will be further evaluated using comparisons with field performance in later sections.

Table 6. Results of Linear Amplitude Sweep tests performed at IT PG specification temperature for $N_{f35\%}$

Binder Name	A	COV	B	COV	Nf 2.5%	COV	Nf 5%	COV
1090-14-70	119565	0.6%	-3.39	0.3%	5344	1.5%	509	2.1%
9040-09-70	484614	6.4%	-3.61	0.5%	17713	4.6%	1449	3.2%
1130-12-71	159162	2.2%	-3.06	0.3%	9684	3.1%	1165	3.7%
1177-10-70	533388	8.5%	-3.41	1.2%	18282	4.8%	1714	2.1%
6590-00-10	252994	2.7%	-3.44	0.6%	13271	0.7%	1224	0.8%
3120-06-70	319036	0.3%	-3.34	0.4%	13892	0.8%	1374	1.7%
9140-07-70	407210	1.8%	-3.17	0.3%	22146	1.0%	2463	0.3%

Table 7. Results of Linear Amplitude Sweep tests performed at IT PG specification temperature for N_{fPeak}

Binder Name	A	COV	B	COV	Nf 2.5%	COV	Nf 5%	COV
1090-14-70	321538	2.4%	-3.39	0.3%	14371	1.5%	1369	0.8%
9040-09-70	524022	3.2%	-3.61	0.5%	19170	5.0%	1570	6.3%
1130-12-71	208107	1.3%	-3.06	0.3%	12661	0.4%	1523	0.2%
1177-10-70	417980	22.6%	-3.41	1.2%	18282	19.1%	1714	16.4%
6590-00-10	309842	3.9%	-3.44	0.6%	13271	1.9%	1224	0.4%
3120-06-70	295981	14.0%	-3.34	0.4%	13892	12.9%	1374	12.0%
9140-07-70	403821	1.5%	-3.17	0.3%	22146	2.4%	2463	3.0%

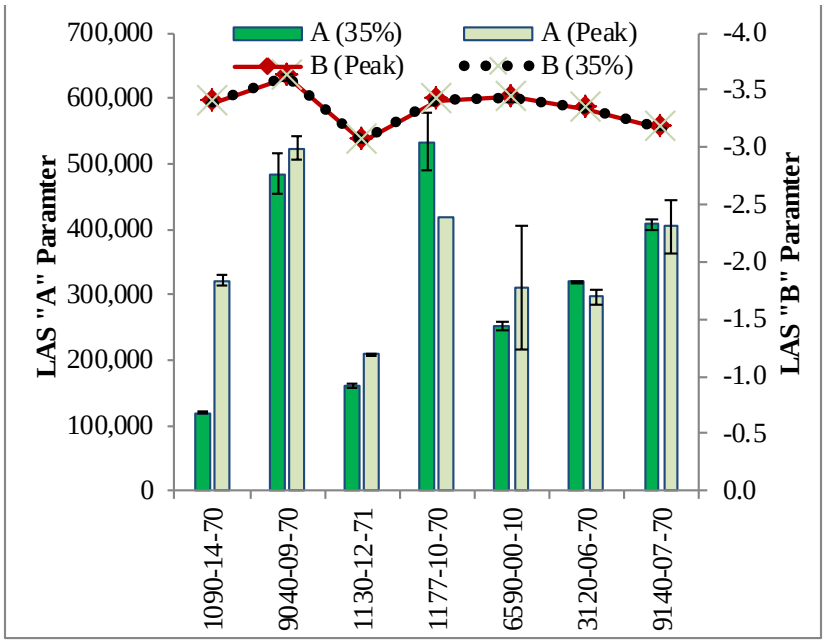

Figure 4. Linear Amplitude Sweep Fatigue Power Law Corefficitents ("A" and "B") using both failure criteria from tests performed at IT PG specification temeprature.

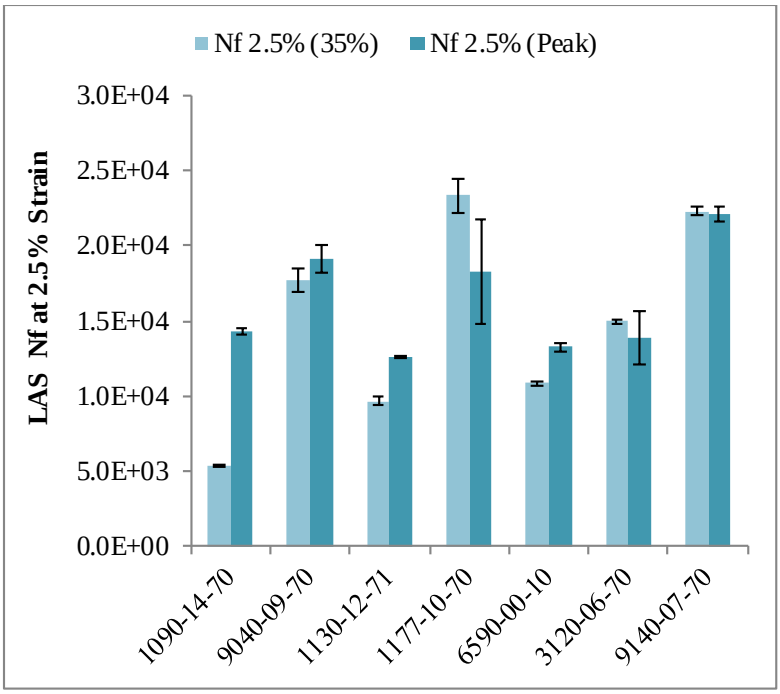

(a)

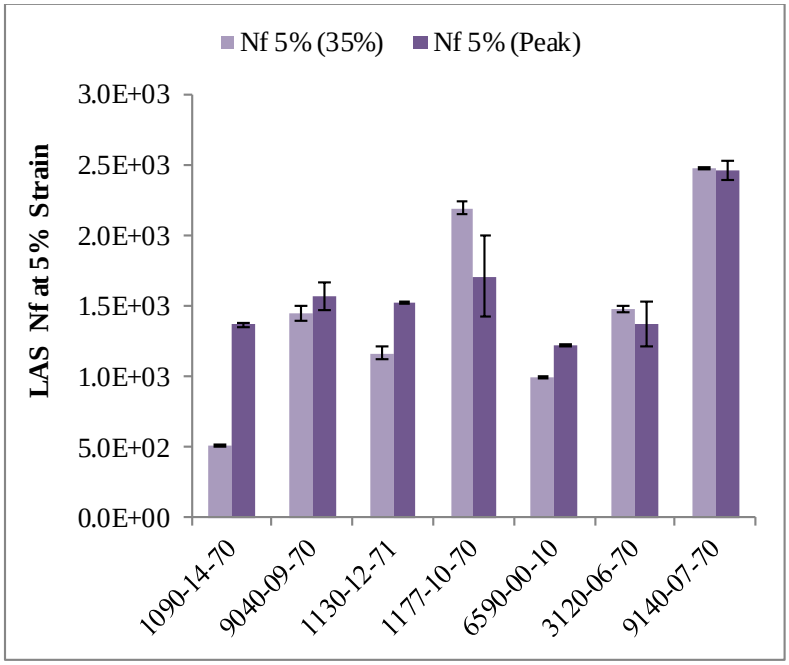

(b)

Figure 5. LAS N_f results using both failure criteria for (a) 2.5% strain, and (b) 5% strain at IT PG specification temperature.

Performance Data

The performance of the monitored field sections in phase I was based on survey carried out between 2004 and 2006, in the latter of which signs fatigue cracking initiation were observed in many sections in the form of longitudinal crack formation, while later stages of crack propagation into alligator cracking was not observed.

As part of the phase II study a condition survey was performed on all sections in October 2012. In this survey it was found that projects 1090-14070, 9040-09-70, 1177-10-70, and 1130-12-71 had been overlaid before the start of phase II. Thus a complete set of field performance data for the fatigue evaluation could not be put together from the 2012 survey results. Furthermore, of all non-overlaid surveyed sections in phase II (including sections not included in phase I fatigue evaluation) only two sections showed signs of fatigue cracking and thus sufficient performance data for a complete fatigue damage data set was not available from the 2012 survey results. As a result it was decided to use the 2006 data for evaluation of the LAS parameters introduced in phase II of the study. Similar to Phase I, the performance index used was based on the percent of 100 ft segments out of the approximately 1.0 mile field section on the project that showed signs of occurrence of fatigue cracking. The total crack length observed per segment were up to 200 ft, with the severest crack widths in the range of ¼ to ½ inches wide. The indexes yielded a wide range of performances for the different field, and thus allowed for clear discrimination between the different sections. The survey results are shown in Table 8, while Table 9 shows a summary of LAS results to be compared to the field performance index.

Table 8. Field performance based on observation of longitudinal cracking.

Project ID	Section ID	Surveyed Cracking Condition
9040-09-70	20090, 160	1 to 100 feet per station / less than 1/2-inch in width
	20100, 110, 120, 130, 140, 150, 170,180, 190, 200, 210, 220	-
9140-07-70	87470, 480 & 490	-
	87500	-
1177-10-70	68660	1 to 100 feet per station / less than 1/2-inch in width
	68670, 680, 690, 700 & 710	-
	68720	1 to 100 feet per station / less than 1/2-inch in width
6590-00-70	116410	-
	116420	1 to 100 feet per station / less than 1/2-inch in width
1130-12-71	54010	1 to 100 feet per station / less than 1/2-inch in width
	54020	NA
	54030, 52250, 52260	101 to 200 ft per station / less than 1/2-inch in width
	54040, 52270	101 to 200 ft per station / less than 1/2-inch in width
	54050, 52290	1 to 100 feet per station / less than 1/2-inch in width
	52280	101 to 200 ft per station / less than 1/2-inch in width
3120-06-70	89150	101 to 200 ft per station / less than 1/2-inch in width
	89160	1 to 100 feet per station / less than 1/2-inch in width
	89170	1 to 100 feet per station / less than 1/2-inch in width
1090-14-70	57950, 135400	1 to 100 feet per station / less than 1/2-inch in width
	57960, 56390, 56400, 56430, 135310, 135320	-
	57970, 57980, 57990, 56410, 135330, 135390, 135410, 135420	1 to 100 feet per station / less than 1/2-inch in width
	56420	-
	135300	1 to 100 feet per station / less than 1/2-inch in width

Table 9. LAS criteria evaluated against field performance tested at 15°C and the IT PG.

Project ID	LAS Nf at 15°C				LAS Nf at IT PG				$\lvert G^* \rvert \sin\delta$ (kPa)	Cracked Segments
	2.5% R-35%	5.0% R-35%	2.5% Peak	5.0% Peak	2.5% R-35%	5.0% R-35%	2.5% Peak	5.0% Peak		
1090-14-70	4283	386	10906	984	5344	509	14371	1369	1226	67%
9040-09-70	16396	1617	14216	1402	17713	1449	19170	1570	2507	14%
1130-12-71	7763	923	8599	1022	9684	1165	12661	1523	2314	100%
1177-10-70	15011	1875	15856	1981	18282	1714	18282	1714	2563	29%
6590-00-70	8070	875	8601	932	13271	1224	13271	1224	3244	50%
3120-06-70	10003	795	12714	1010	13892	1374	13892	1374	2391	100%
9140-07-70	15746	1882	16488	1969	22146	2463	22146	2463	2419	0%

Using the data summarized in Table 9 a set of correlation graphs were created to investigate the relationship between the test results and field performance, as shown in Figure 6, Figure 7 and Figure 8. Figure 6 shows no between |G*|sinδ at RTFO conditions and field performance, indicating the unsuitability of using this parameter for evaluating the modified binders used in the present study. From Figure 7 and Figure 8 it can be seen that in all conditions and for all evaluated parameters a general trend is observed in which reduction in the LAS Nf value has led to increased field cracking.

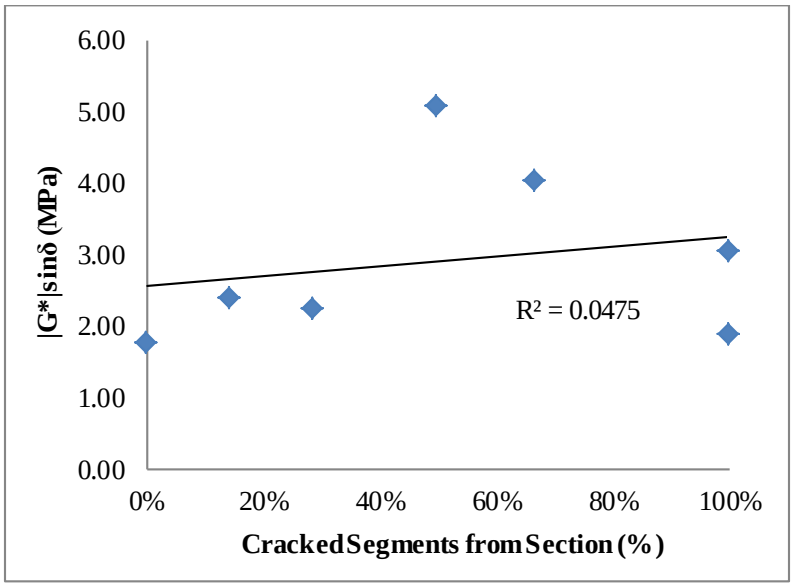

Figure 6. Relationship between field performance and the |G*|sinδ

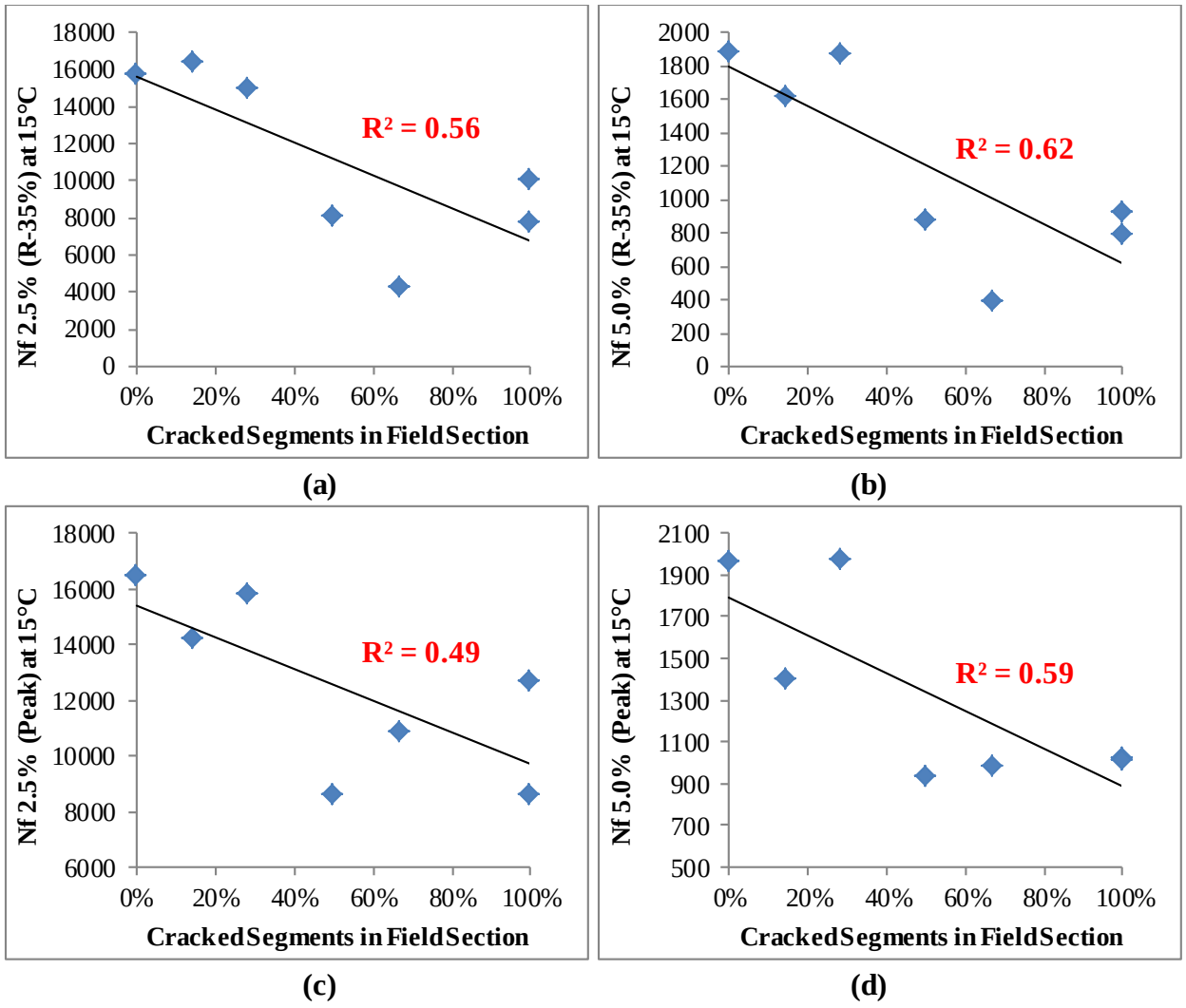

Figure 7. Relationship between field performance in terms of percent cracked segments per field section and LAS parameters from tests at 15°C

In terms of correlation, the best relationship was established between the LAS tests performed at the local climate intermediate PG temperature using the Nf at peak criterion. By minimization it was observed that the highest correlation was achieved if an input strain level of approximately 2.5% was used. Optimally the input strain would be determined as a function of the pavement thickness, thus for binders to be used in thicker pavements a smaller input strain would be necessary, while larger input strains would be necessary for binder evaluation for a thin

pavement layer. For the set of field sections evaluated in the present study, the pavement layer thicknesses for five of the sections were between 4.5 to 6 inches. The two sections with layer thicknesses less than 4.5 inches were overlaid on existing pavement, thus the layer deflection and input strains are expected to be similar to that of thicker pavements. Thus overall, the studied sections are believed to all have relatively thick layers, thus use of a constant and lower input strain level would seem appropriate.

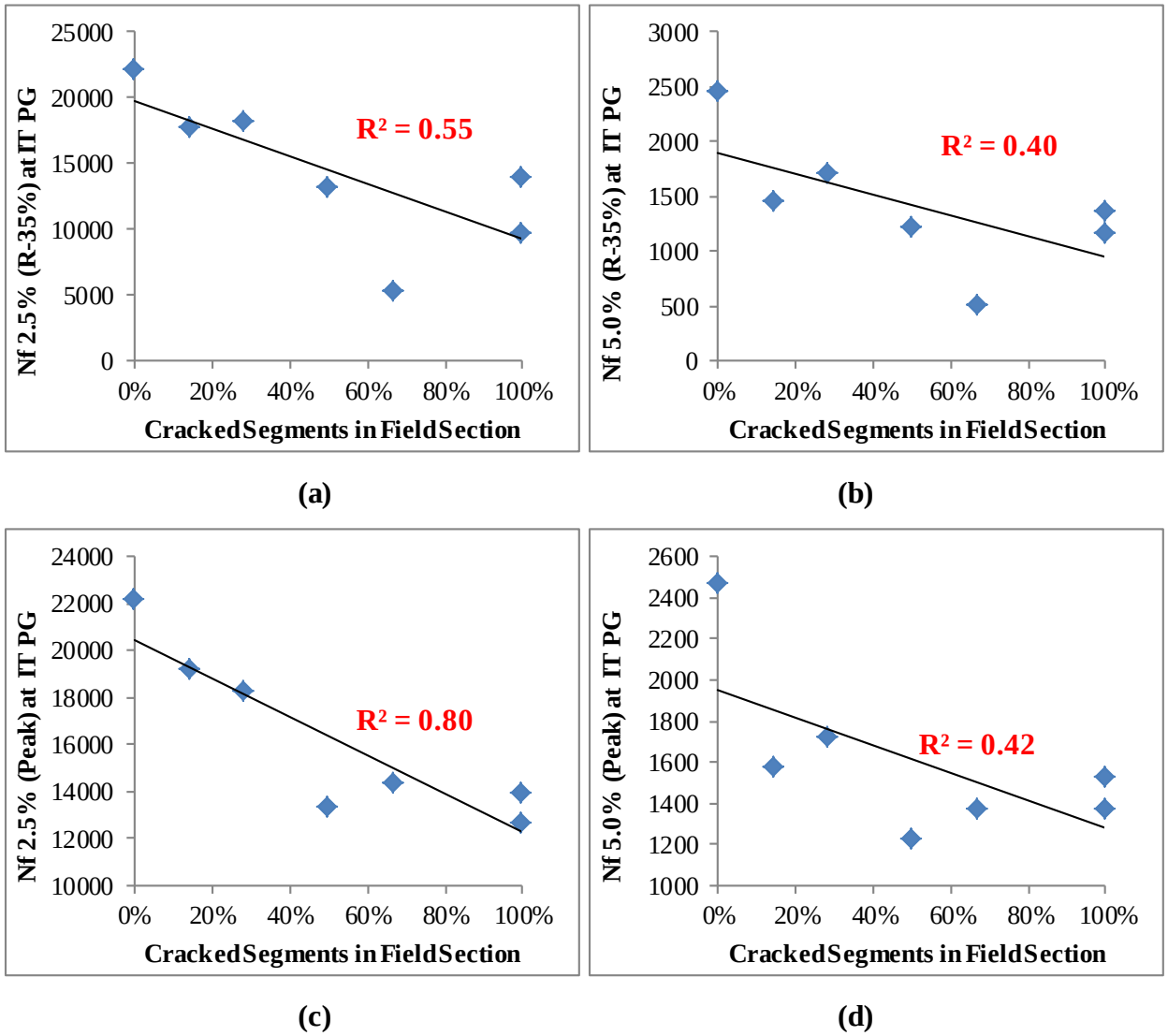

Figure 8. Relationship between field performance in terms of percent cracked segments per field section and LAS parameters from tests at IT PG temperature

An important aspect that was noted in analysis of the performance data was the significant difference in ESALs applied to the different pavements over the analysis period. In order to account for the varying number of load applications to each binder, it was decided to estimate the number of ESALs until 75% of the segments in all sections showed fatigue cracking signs, by extrapolating from the last 2 damage and traffic data available. Thus the number of ESALs to a constant damage level could be directly compared to the LAS Nf and thus take out the traffic variable between data points. The process is shown in Figure 9 and results are summarized in Table 10.

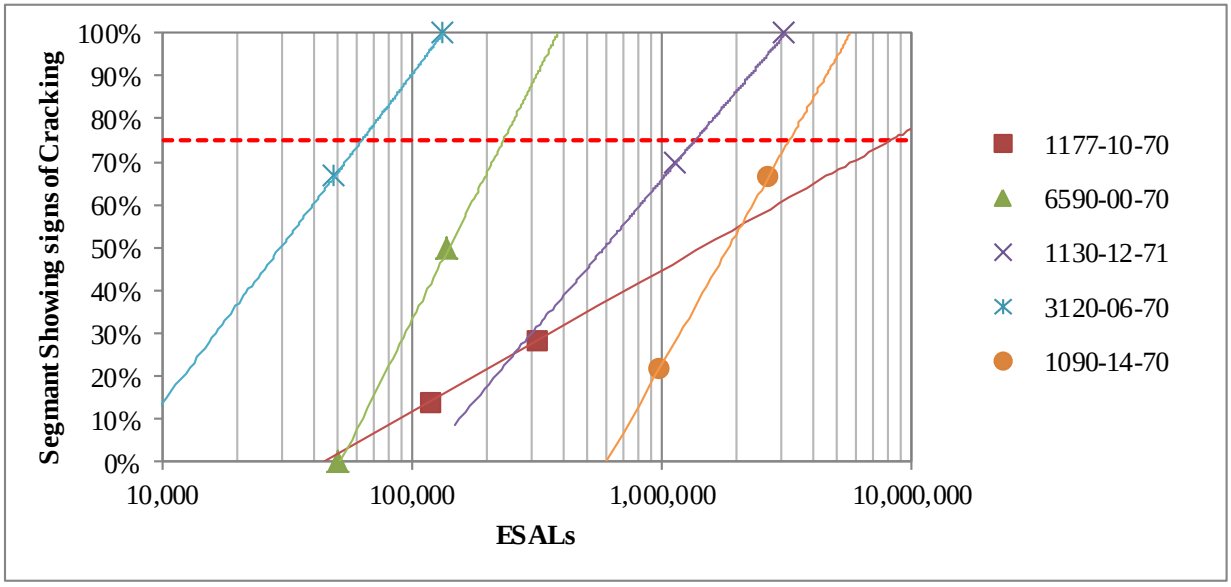

Figure 9. Estimation of number of ESALs to a fixed damage level in all sections

Table 10. Number of ESALs corresponding to 75% of segments in section showing fatigue damage

Project ID	Total ESALs to Full Damage
1090-14-70	3,231,745
1130-12-71	1,356,007
1177-10-70	8,227,689
6590-00-70	231,567
3120-06-70	62,790

It should be noted that sections 9040-09-70 and 9140-07-70 were eliminated due to the very limited to no damage in these sections resulting in estimated near infinity ESAL numbers for the ultimate damage conditions. Comparing the above ESAL values with the Nf from the LAS fatigue power law using the "A" and "B" parameters derived previously, new correlations are made with field performance, as shown in Figure 10. As described, the tests are conducted at the corresponding intermediate temperature (IT) as determined from the local climatic conditions, and using the estimated traffic that would cause a constant damage level to account for the effect of traffic level variation between sections.

Although the primary emphasis of the study and the purpose of the LAS test is to differentiate binders based on their damage resistance, this ability also creates the potential to develop criteria limits and specification for binder selection to minimize expected fatigue damage. To use the LAS as a binder selection test a single strain value will need to be used dependent on the pavement structure (weak or strong) and different N_f limits are simply used for various ESAL ranges, either based on pavement mix design categories (i.e. E-0.3, E-3, etc.), or AASHTO MP-19 grade designations (i.e. "S", "H", "V" and "E" grades). A set of estimated limits for N_f are proposed in Table 11 based on the relationship derived in Figure 10. Although

the observed trend and the suggested limits clearly demonstrate the potential ability of the LAS test for derivation of performance based specification limits, the current values suggested in Table 11 based on RTFO-aged conditions should be considered preliminary.

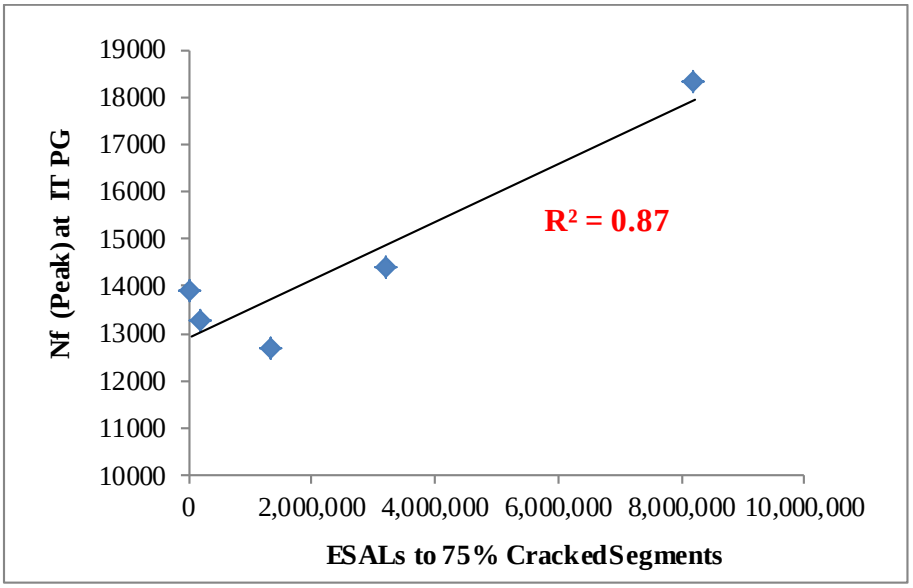

Figure 10. Relationship between field performance and LAS parameters by comparing to the number of ESALs in the field to a fixed damage level

Table 11. Suggested preliminary LAS minimum N_f limits for pavement design based on mixture category and AASHTO MP-19 grade

ESALs	Mix Design Category	Minimum LAS Nf Required (RTFO Condition)
300,000	E-0.3	13000
1,000,000	E-1	14000
3,000,000	E-3	15000
10,000,000	E-10	19000
30,000,000	E-30	31000

ESALs	Design Grade	Minimum LAS Nf Required (RTFO Condition)
3,000,000	S	15000
10,000,000	H	19000
30,000,000	V, E	31000

It must be noted that due to extreme limitations in the quantity of available material, PAV aging of the binders was not feasible, thus as previously mentioned, all tests were conducted on RTFO-aged samples. As the field condition data represents only 3 years of performance, the comparisons made with RTFO aged material is expected to be representative in the present conditions. Nonetheless, binder fatigue characterization is often conducted on PAV-aged material, thus data available from previous studies was used to conduct a comparison between LAS N_f results from binders with RTFO aging with those that have been conditioned using the PAV. The comparison is shown in Figure 11, in which it can be seen that for the multiple binder sources (including LTPP binders 370901, 090960, 350903, 370964, and 04B903) and various modification levels and different test temperatures, a close relationship exists between the results at both aging levels, even after removing the large data point from the trend line.

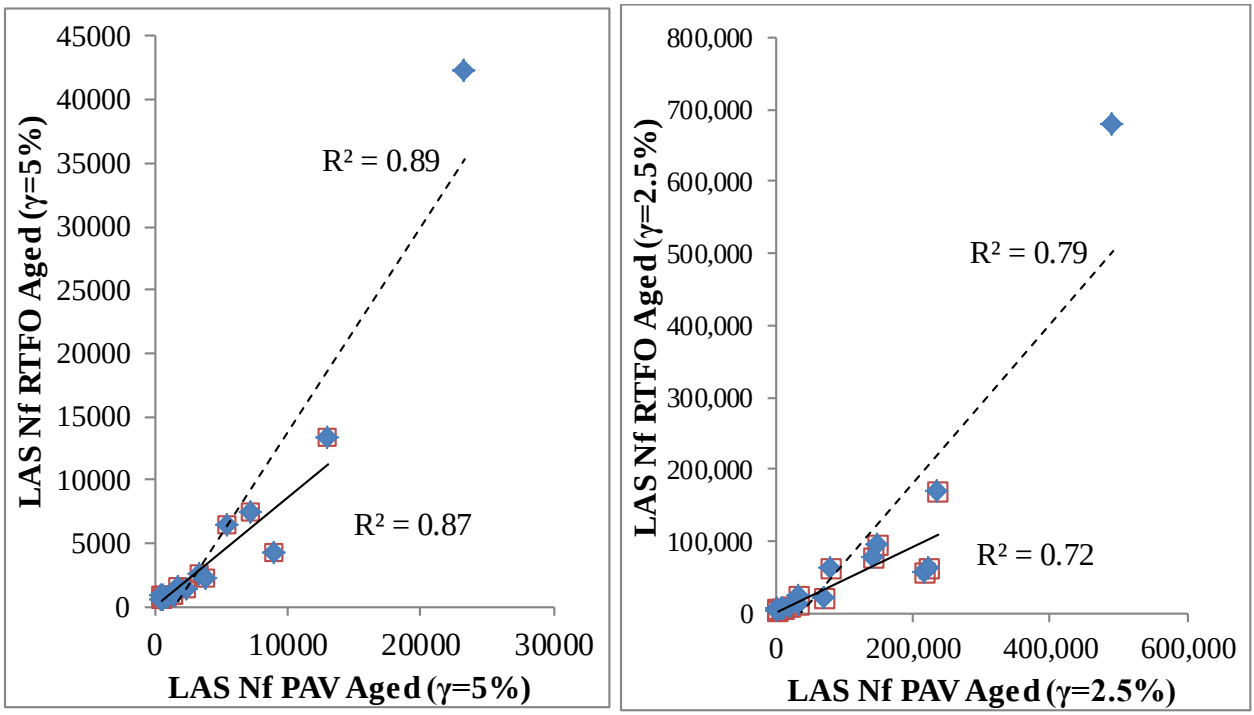

(a) **(b)**

Figure 11. Comparison between LAS results at two strain levels at RTFO and PAV aged conditions (solid trend line shows trend after removal of large data value)

Although the observed relationship between RTFO and PAV aged LAS response is not expected to be necessarily applicable to any binder source and modifier, the existence of a strong correlation between the two conditions would suggest that a set of LAS minimum N_f limits specified in Table 11 should also be derivable for PAV aged binders. For example, if the relationship shown in Figure 11 was used to adjust the limits in Table 11 to reflect estimated values at PAV conditions, the limits shown in Table 12 may be derived. It must be re-emphasized that these limits are only an estimated example, thus actual limits for possible use in future specification will need to be based on PAV-aged test data from a larger set of binders.

Table 12. Estimated LAS minimum limits at PAV conditions used to demonstrate expected potential for dervinig such limits based on PAV-aged LAS tests

ESALs	**WisDOT Mix Design Category**	Minimum LAS N_f Required (PAV Condition)
300,000	E-0.3	28000
1,000,000	E-1	30000
3,000,000	E-3	33000
10,000,000	E-10	41000
30,000,000	E-30	67000
ESALs	**AASHTO MP-19 Grade**	Minimum LAS N_f Required (PAV Condition)
3,000,000	S	33000
10,000,000	H	41000
30,000,000	V, E	67000

Another noteworthy factor is that the pavements sections used in this study likely contain a percentage of reclaimed asphalt pavement (RAP) materials, which will replace a portion of the mixture's total binder content and thus affect the ultimate properties of the fresh binder in the pavement. This effect can be very complex when factoring in the uncertainties with regards to the blending efficiency and level between the RAP binder and the virgin binder and the various

RAP sources likely used. Thus in the present study the fresh binder retained from these projects during construction was used and the complexity of the possible effect of RAP binder replacement was not included in the scope of the research project. Future studies may need to include extracted and recovered binders from the monitored field sections to further investigate this issue.

Proposed Procedure for Fatigue Evaluation (LAS)

1. Prepare and load 8 mm DSR sample in accordance to AASHTO T 315 (DSR).
2. Condition sample for 15 minutes at the required intermediate temperature performance grade criterion for the project location, in accordance to AASHTO M 320.
3. Perform a single loading sequence consisting of one frequency sweep step at 0.1% strain between 0.1 to 30 Hz, followed by a strain sweep at 10 Hz between 0.1 and 30% over 3100 cycles (total loading approximately 6 minutes).
4. Copy frequency, complex modulus, phase angle, and storage modulus from DSR output to analysis spreadsheet for automatic calculation of "B".
5. Copy time, complex modulus, phase angle, stress, and strain from DSR output to analysis spreadsheet for automatic calculation of "A" at damage corresponding to peak.
6. Use resulting fatigue law ($Nf = A\gamma^B$) to calculate Nf at the target strain level (γ). Use γ=2.5% for strong pavement with surface layers thicker than 4.5" (or overlays) and γ=5.0% for thinner pavement layers.
7. Compare N_f to the minimum allowable N_f limits in Table 11 based on mix design category or AASHTO MP 19 grade. Fail binders with N_f values lower than the allowable limit.

Note 1: The N_f corresponding to the damage at the peak stress is the result of the Visco-elastic Continuum Damage (VECD) analysis performed automatically by the analysis spreadsheet and is not equivalent to the number of test cycles (or strain) at the peak stress. This is highlighted by the lack of correlation between the N_f and the strain at peak shown in Figure 12. Thus it is necessary to use the analysis spreadsheet for meaningful interpretation of the LAS test results.

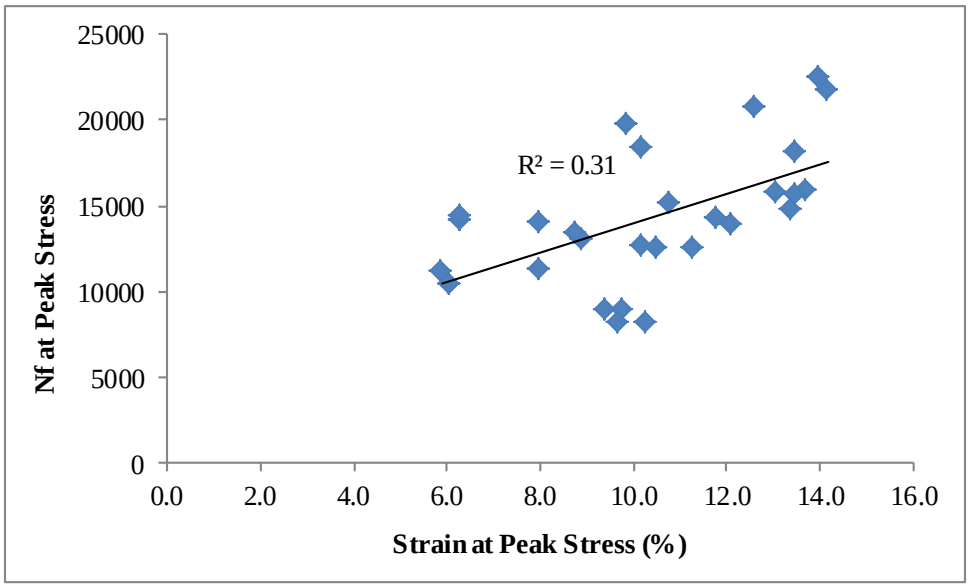

Figure 12. Lack of correlation shows that N_f at peak stress should not be assumed equivalent to the strain at peak stress

Summary and Conclusions for Binder Fatigue Evaluation

In this section the Linear Amplitude Sweep (LAS) test, standardized under AASHTO TP101, was considered and evaluated as a potential test for assessment of binder resistance to fatigue cracking. The following points summarize the main findings:

- In phase I it was shown that the Np20 parameter derived from the time sweep test can relate well to the observed field performance. Since then, this test has been replaced with

the Linear Amplitude Sweep (LAS), due to the former test being time-consuming and having repeatability issues.

- The Superpave |G*|sinδ parameter was found to relate poorly to the field performance of the modified binders investigated in the current study. Therefore the replacement of this parameter is needed to control binder fatigue resistance.
- Comparison of LAS results to field performance indicated that the best relationship is achieved when the test is performed at the intermediate temperature PG based on the project location climate in accordance to AASHTO M320.
- Two failure criteria were evaluated for calculation of the "A" parameter in the LAS fatigue power law. It was shown that both criteria resulted in correct trends and fair to very good correlations with field performance. The best correlations were found using the Nf corresponding to the damage level at the peak stress, and when they are adjusted for effect of the traffic volume (ESALs) for the sections.
- It is recommended as a future activity that the use of |G*|sinδ results for derivation of the LAS "B" parameter be investigated. This would allow for conducting the LAS test on the same sample as the PG test by simply adding a strain sweep step after the conclusion of the |G*|sinδ loading cycles.
- A set of preliminary minimum allowable LAS Nf limits and a test procedure have been developed and suggested based on the results at RTFO aged conditions, and estimated for the PAV-aged conditions. The limits show the clear potential of this procedure for usage as a fatigue performance-based specification test. Further testing at different aging conditions or using field extracted binders will be needed to derive finalized limits for possible use in future WisDOT specification.

- Based on the results of phase I and phase II analyses, the Linear Amplitude Sweep test performed at the required Superpave intermediate temperature grade of the project location, and the resultant Nf at peak stress parameter, are recommended for use for evaluation of modified binder fatigue damage resistance.

CHAPTER THREE: RESISTANCE TO THERMAL CRACKING

Background

In phase I of this project the Direct Tension Test (DTT) and the Bending Beam Rheometer (BBR) were used to evaluate the studied modified binders in terms of field thermal cracking damage. DTT testing was abandoned in phase I after poor repeatability was observed and the average tensile stress and strain at failure of four tested binders was used for calculation of the critical cracking temperature for all of the tested binders. Although an acceptable relation was found between the critical cracking temperature using the stress criterion and field performance, the reliance of the data on non-binder specific average DTT values, and the current general lack of use of DTT in the industry make use of this parameter unpractical as a Wisconsin guideline and binder selection criteria.

Phase I tests also included the current Superpave specification utilizing the BBR. A decent reliability was achieved between S(60) and performance after removal of field data for which a chance of reflective cracking existed, significant cracking was still observed for binders both passing and failing the S(60) criteria. The BBR characterizes binders in the linear viscoelastic domain using small stress and strain values, potentially not accounting for the greater damage resistance capability of modified binder as well as post peak load resistance that is commonly seen in such binders.

The BBR-SENB test was developed by MARC under the Transportation Pooled Fund study on Low Temperature Cracking, sponsored by WisDOT, for thermal cracking characterization (Velasquez, et al., 2011; Bahia, et al., 2012). The BBR-SENB test geometry is based on ASTM E399. Previous tests based on the 3-point bending of notched asphalt beams

have been previously used by other researchers (Chailleux & Mouillet, 2006; Hesp, 2003; Hoare & Hesp, 2000), but none were based on the modification of the current BBR setup which is widely available in labs across the state. Asphalt binders samples prepared using the BBR geometry with an added notch are tested in a three-point bending setup, loaded at a constant rate of displacement thus allowing for observation of post failure behavior.

The test uses a modified Bending Beam Rheometer (BBR), with the addition of a loading motor that controls the displacement rate during testing, a load cell with a higher capacity than the regular BBR, and modified beam placement fixtures, as shown in Figure 13. Tests were run at a constant displacement rate of 0.01 mm/sec in this study. In the BBR-SENB analysis, the failure energy, G_f is calculated instead of G_{IC} parameter defined in Linear Elastic Fracture Mechanics. Failure energy is defined as the total area under the entire load-deflection (P-u) curve, divided by the area of the ligament, as shown in equation 7. The displacement at failure, u_f, is also reported as a characterization parameter from this test procedure.

$$\boldsymbol{G_f = \frac{W_f}{A_{lig}} = \frac{\int P du}{A_{lig}}} \qquad (7)$$

Where:

- W_f is work of failure,
- G_f is failure energy
- P and u are the load and displacement measured by the BBR-SENB,
- A_{lig} is the area of the ligament

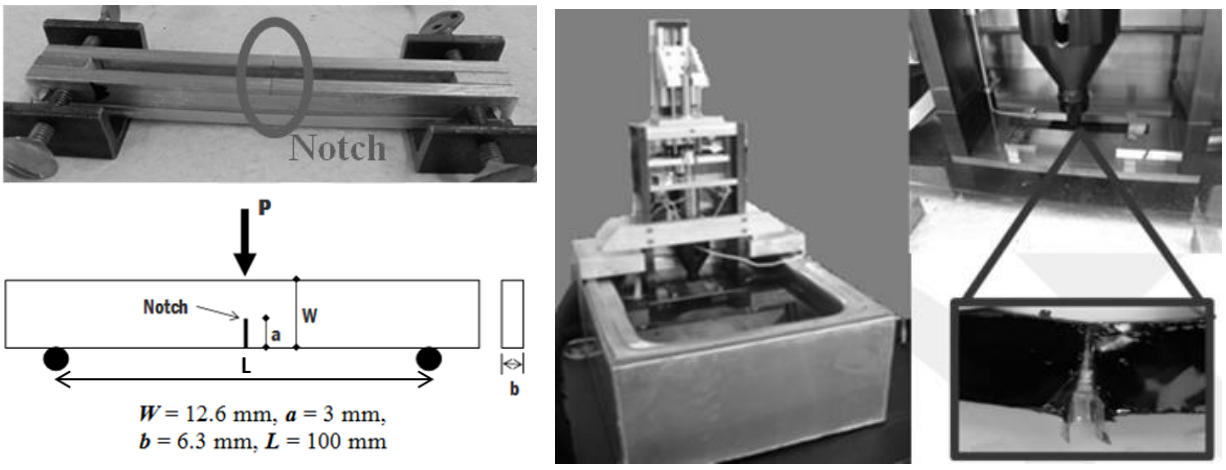

(a) **(b)**

Figure 13 (a) BBR-SENB sample mold and dimensions, and (b) BBR-SENB loading device and setup.

A draft AASHTO procedure has been reviewed by the FHWA binder ETG and is currently under consideration by AASHTO for provisional standardization. The test has been evaluated using a wide range of binders, including binders from LTPP sections to ensure representability of the procedure results (Bahia, et al., 2012). This test has been proposed as a low temperature failure test to fill the current void left by the DTT with a practical and more repeatable procedure.

Selected Projects

Low temperature damage in the form of transverse cracking was measured as part of the condition survey conducted as part of the phase II study. A number of the sections that were previously evaluated in phase I had been overlaid before phase II and thus were unusable in the phase II study. Fortunately the remaining sections, as well as a number of sections not considered in phase I showed wide range of thermal cracking performance and thus a viable sample set of performance data could be derived from the 2012 survey.

Sections 9140-07-70, 6590-00-70, 4100-10-71, and 3120-06-70 from phase I had not been overlaid and was thus included in the phase II sample set. Sections 1170-13-70 and 7132-04-61 were added to the sample set in phase II. The binder in section 4100-10-71 was unmodified and was thus used as a control section. Further information corresponding to the selected sections is shown in Table 13. The average annual minimum air temperatures were derived from LTPPBind v3.1.

Table 13. Information corresponding to selected field section for thermal cracking binder evaluation

Project Name	County	DOT Project ID	Binder	Year of Construction	Average Annual Low Temperature
USH 51	Iron	1170-13-70	64-34	2004	-32.1°C
STH 64	Langlade	9140-07-70	58-34	2003	-31.2°C
STH 93	Buffalo	7132-04-61	64-28	2004	-31.2°C
STH 110	Waupaca	6590-00-70	64-28	2003	-29.8°C
STH 67	Walworth	3120-06-70	64-28	2003	-27.0°C
USH 151	Manitowoc	4100-10-71	64-22 (neat)	2003	26.7°C

Binder Testing

The BBR-SENB binder test was performed in addition to the tests performed in phase I (BBR, DTT, and Tg). In phase I inconclusive results were achieved from the use of the tests performed. Table 14 shows the critical cracking temperatures derived from the tests performed on phase I binders also used in phase II. As the BBR critical temperature was found to be controlled by the stiffness (S(60)) in all binders, the m-controlled critical temperature is not included.

Table 14. Summary of critical temperature values derived from phase I tests

Project ID	T_c S(60) Criterion (°C)	T_c Stress Criterion (°C)	T_c Strain Criterion (°C)	T_g (°C)
9140-07-70	-37	-37	-45	-32
6590-00-70	-32	-31	-58	-31
3120-06-70	-33	-32	-41	-35
4100-10-71	-27	-25	-47	-23

Single Edged Notched Beam Testing

The BBR-SENB test was performed at both -18 and -24°C, the two temperature corresponding to the passing low temperature PG testing temperatures of the field climatic conditions, for each section. The results showed a significant spread and good repeatability, as can be seen in Figure 14. Furthermore it can be seen that the neat binder (4100-10-71) is clearly discriminated from the modified binders, both in terms of G_f and u_f.

Figure 15 compares the BBR-SENB results with the critical cracking temperatures derived from the crossing of the thermal stress and strain from the BBR and the Tg test with the total average DTT failure envelope. In phase I it was found that only the S(60) criterion and the stress criterion provided critical temperatures that were relatable to field performance. As the stress criterion requires the use of the DTT test which is no longer in production due to repeatability issues (as was experienced in phase I), only the S(60) critical temperature was used for comparison with the BBR-SENB data in phase II. The BBR-SENB is considered a simple and convenient replacement for the DTT. It can be seen in Figure 15 that the S(60) criterion Tc seems to approximately follow the BBR-SENB trend, but both of the BBR-SENB parameter provide a much clearer discrimination between the binders, especially with regards to the unmodified binder (4100-10-71), compared to the BBR T_c parameter.

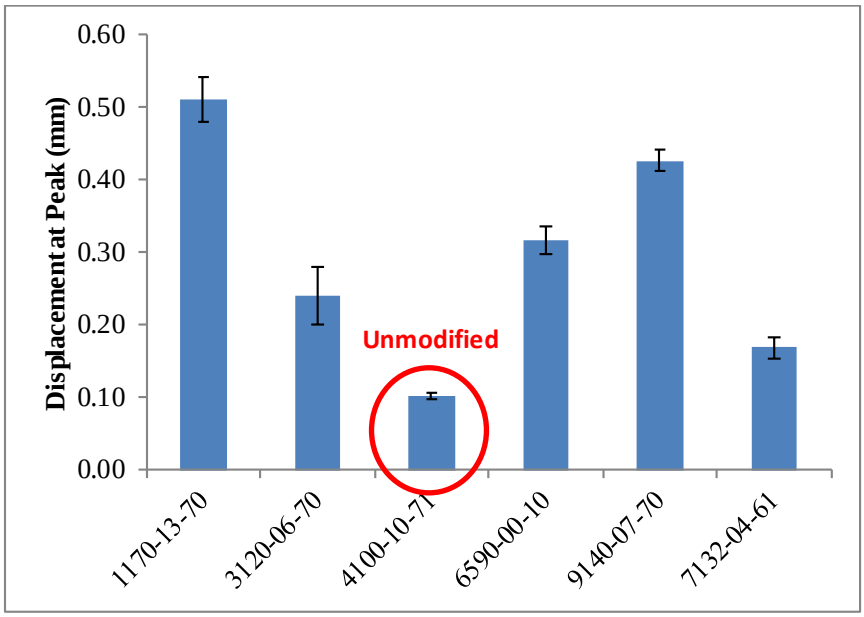

(a)

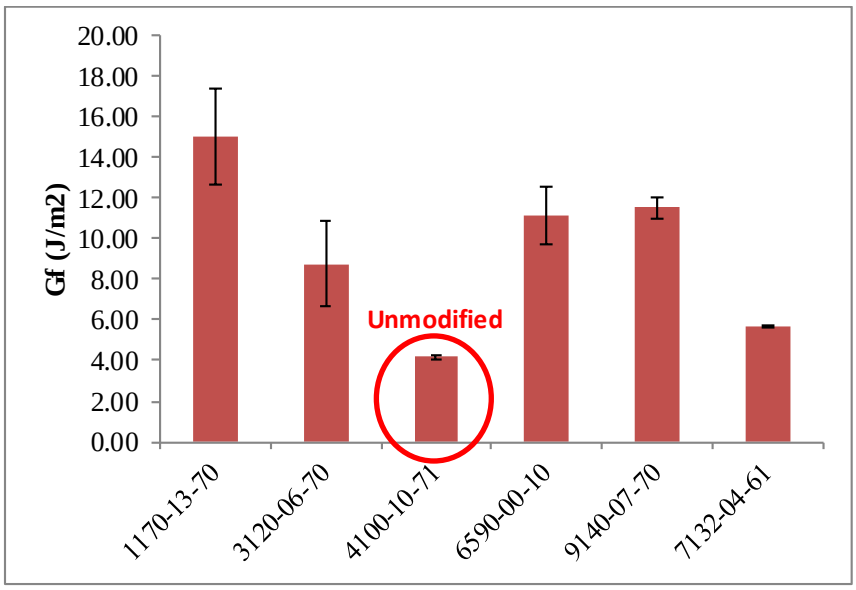

(b)

Figure 14. BBR-SENB results from on selected field section binders at -18°C

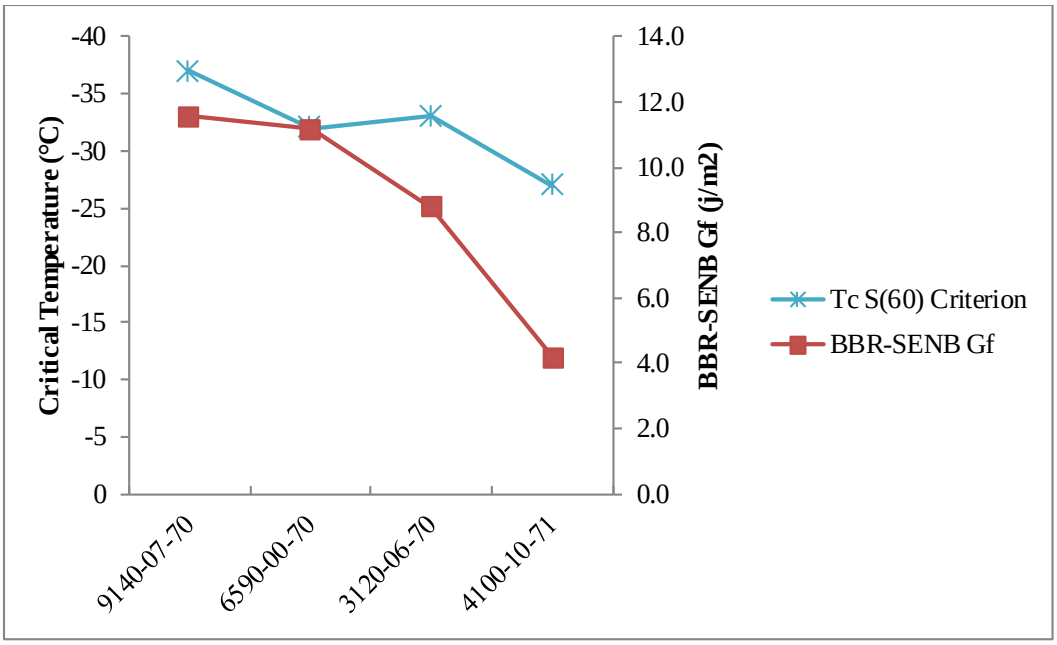

(a)

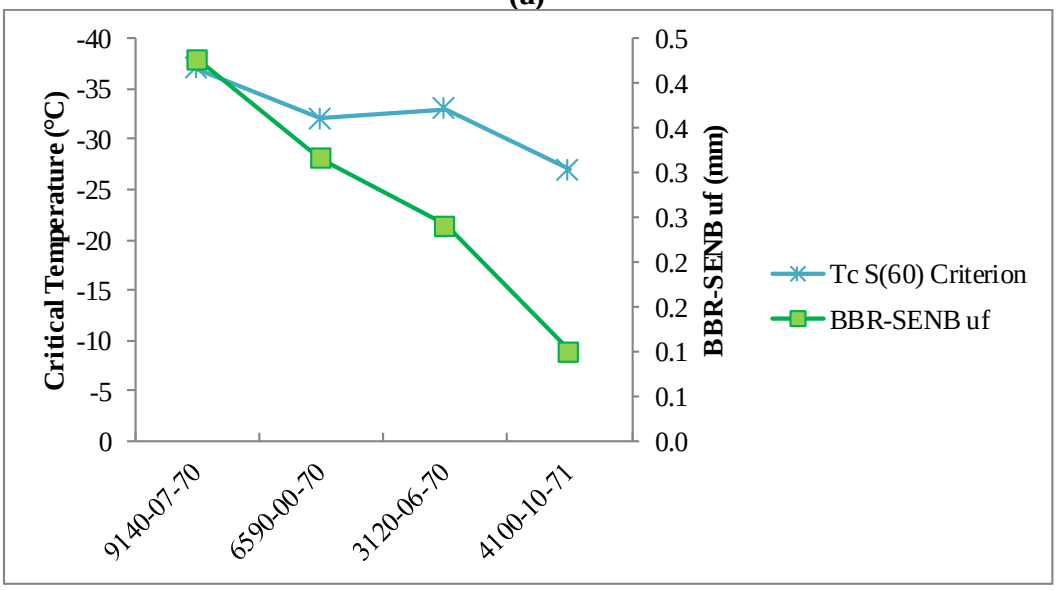

(b)

Figure 15. Comparison of trend between BBR-SENB results and BBR T_c temperatures

Performance Data

As previously discussed, a set of field sections with a wide range of thermal cracking performance were selected for the field performance evaluation of the BBR-SENB test. A summary of the performance from the 2012 survey conducted in phase II, and a comparison to

the PCI values from phase I (2006) are shown in Table 15. The table shows the deduct values due to the presence of thermal cracking at combined severity levels.

Table 15 List of projects showing thermal related cracking, corresponding deduct values from ASTM D6433, binder grade, and average annual low temperature.

	Construction Year	Thermal Cracking (2006)	Thermal Cracking (2012)	Binder Grade	Average Annual Low Temperature
1170-13-70	2003	9	10	64-34	-32.1°C
9140-07-70	2003	0	17	58-34	-31.2°C
7132-04-61	2004	0	44	64-28	-31.2°C
6590-00-70	2003	0	0	64-28	-29.8°C
3120-06-70	2003	6	27	64-28	-27.0°C
4100-10-71	2003	11	41	64-22 (neat)	-26.7°C

Section 6590-00-70 was the only section not showing in thermal cracking damage, as had also been indicated in the 2004 and 2006 surveys in phase I. It interesting to note that the average annual minimum temperature for the project location actually exceeded that of the Superpave PG of the uncracked 6590-00-70 binder. Furthermore, for the case of 3120-06-70 the minimum air temperature was within the allowable temperature range for a 64-28 PG, but the section still displayed a significant amount of cracking. These comparisons highlight the need for additional parameters and criteria for evaluation of the thermal cracking resistance of binders, especially when modified.

Figure 16 and Figure 17 show the relation between BBR-SENB G_f and u_f failure parameters and the measured field thermal cracking PCI at two testing temperatures, with the first being at -18°C, while the later uses the interpolated results (between -18 and -24°C) at the local required low performance temperature as determined by LTPPBind at the 98% reliability level. It can be seen that a relatively good relationship is established, especially with G_f, showing that the BBR-SENB parameters were able to clearly discriminate between the well-performing

and the poorly performing sections. Furthermore the results show an approximately 500% spread in the results.

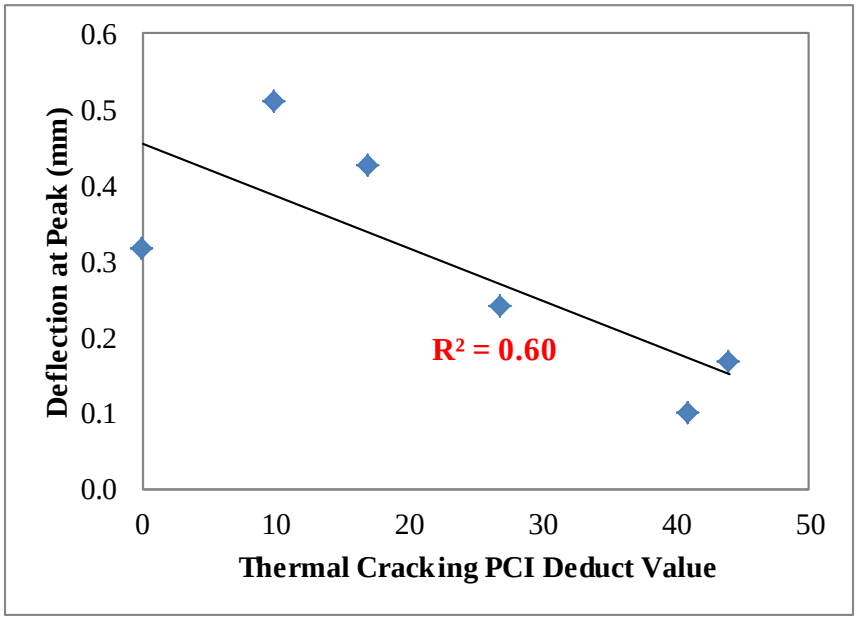

(a)

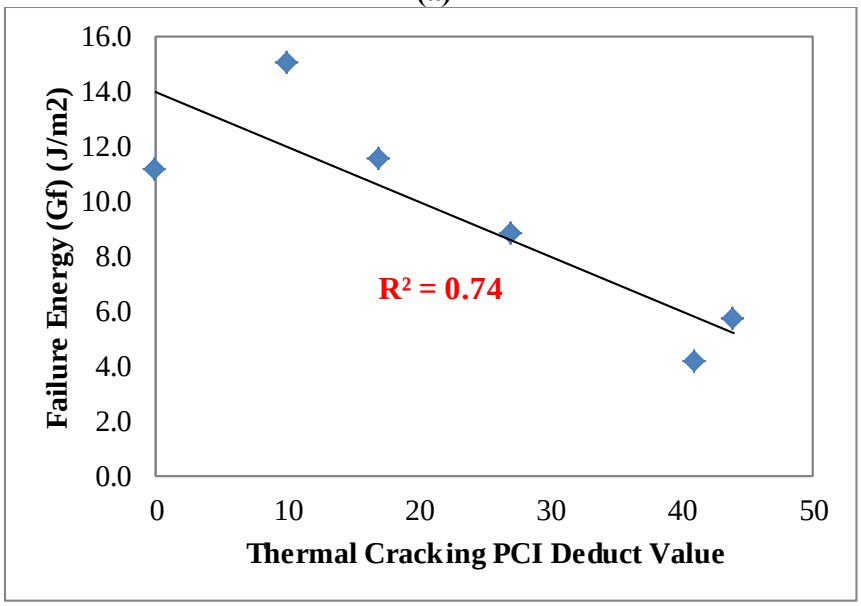

(b)

Figure 16. Comparison of BBR-SENB failure parameters with field section thermal cracking PCI (larger deduct value = higher quantity and/or severity of thermal cracking)

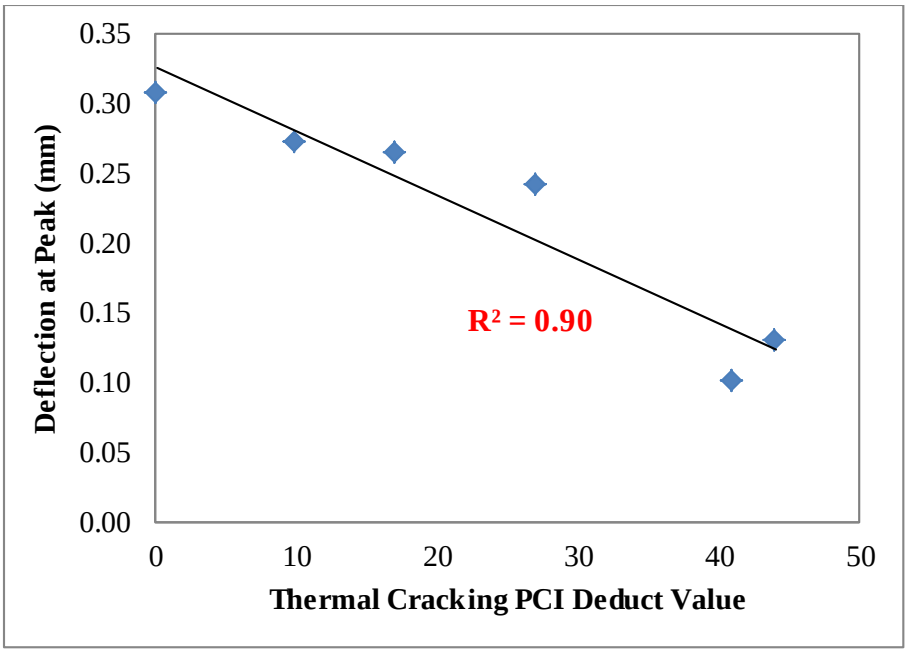

(a)

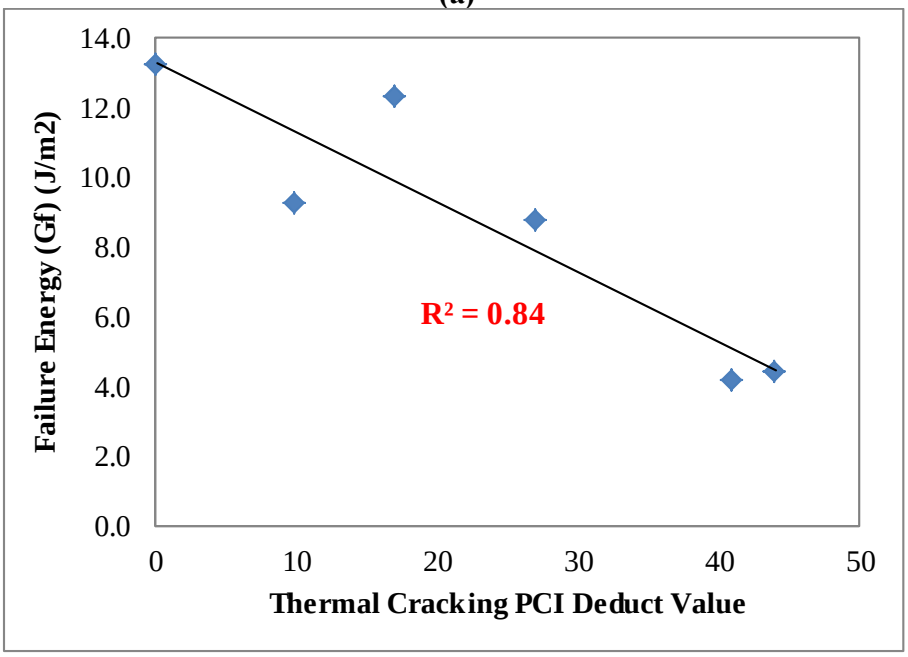

(b)

Figure 17. Comparison of BBR-SENB failure parameters with field section thermal cracking PCI at the exact LTPG temperature (larger deduct value = higher quantity and/or severity of thermal cracking)

Figure 17 indicates that the best relationship between field performance and BBR-SENB results at RTFO-aging conditions is derived when the test is conducted at the local required performance grading low temperature. The present results are in good agreement with previous results from phase II of the Low Temperature Pooled Fund study using comparison of BBR-SENB values to LTPP performance (Bahia, et al., 2012), as well as comparison with field performance in sections in Minnesota (Marasteanu, et al., 2012), indicating the possibility of defining limiting values for the BBR-SENB G_f and u_f to minimize the potential for thermal cracking. Based on the results of this study and data from the LTPP and Pooled Fund studies (Table 16) a failure criterion for the BBR-SENB results is defined as shown in Figure 18. The relationship, $G_f = 25\times(1 - 4\times u_f)$, is shown to be able to differentiate between binder results at temperatures that showed high amounts of thermal cracking for the corresponding binders at RTFO-aged conditions.

Table 16. List of Pooled Fund and LTPP binders used for preliminary criteria development (Bahia, et al., 2012; Marasteanu, et al., 2012)

Binder Grade	Source	Description/Code
PG 58-28	LT Pooled Fund Study	MN County Roud 112
PG 58-28	LT Pooled Fund Study	MN County Roud 112
PG 58-28	LT Pooled Fund Study	MN County Roud 112
PG XX-34	LT Pooled Fund Study	MN County Roud 112
PG 64-22	LTPP Material Library	350902
PG 58-22	LTPP Material Library	350903
PG 64-22	LTPP Material Library	340901
PG 76-22	LTPP Material Library	370964
PG 64-22	LTPP Material Library	370963
PG 58-28	LTPP Material Library	340902
PG 76-22	LTPP Material Library	370962
PG 78-28	LTPP Material Library	340961
PG 76-22	LTPP Material Library	370960
PG 64-22	LTPP Material Library	370901

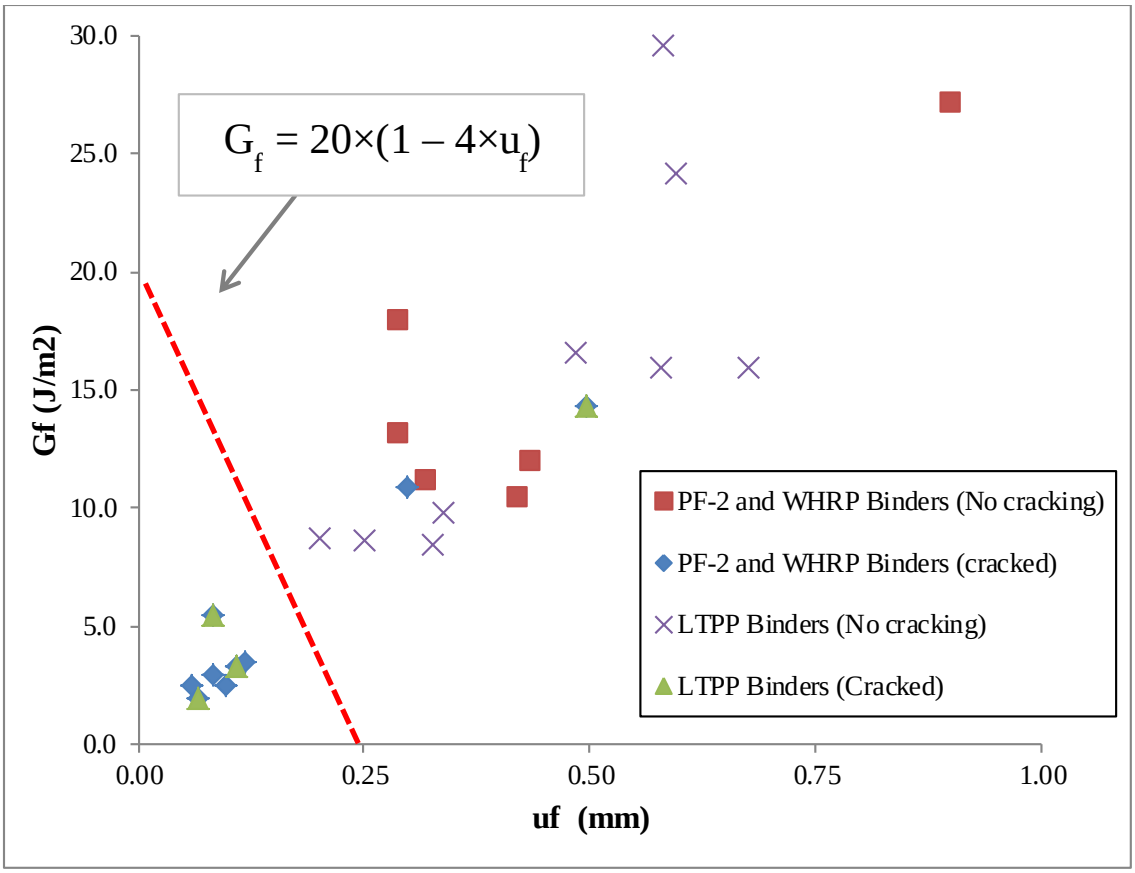

Figure 18. BBR-SENB proposed preliminary specification graph at RTFO-aged conditions (lower left triangle fails the specification)

As previously discussed for the Linear Amplitude Sweep procedure, although testing at PAV-aged conditions was not possible due to the lack of sufficient materials from phase I of the study, a conclusive suggestion of actual specification limits based on the BBR-SENB test will require comparison to PAV-aged binder conditions, as used in the current Superpave Low Temperature Characterization procedure. To this end a comparison between a limited number of BBR-SENB results from LTPP binders (370964, 090960, and 04B903) and Asphalt Research Consortium sources at two aging conditions and different testing temperatures is shown in Figure 19.

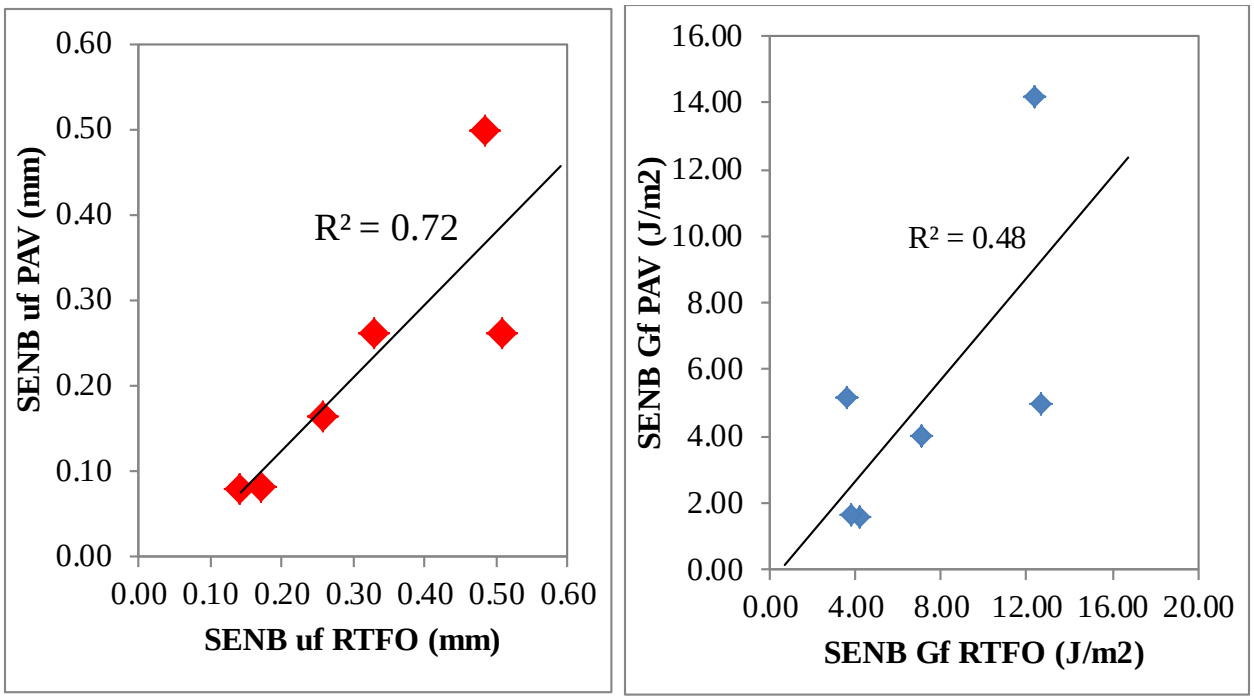

(a) **(b)**

Figure 19. Comparison between BBR-SENB results at RTFO-aged and PAV-aged conditions for (a) failure deflection, and (b) failure energy.

Although the present data is not sufficient to discern more than a general trend between the two aging conditions, the limited data suggests that specification limits similar to that shown in Figure 18 using the RTFO-aged sample can also be developed for PAV-aged materials. An example of how such a relationship would look using the relationships in Figure 19 is shown in Figure 20. It is observed that the data points are closer to the origin, while the same failure limit as used for the RTFO-aged condition in Figure 18 can be used for the estimated PAV-aged conditions, although it will be much more conservative for this condition.

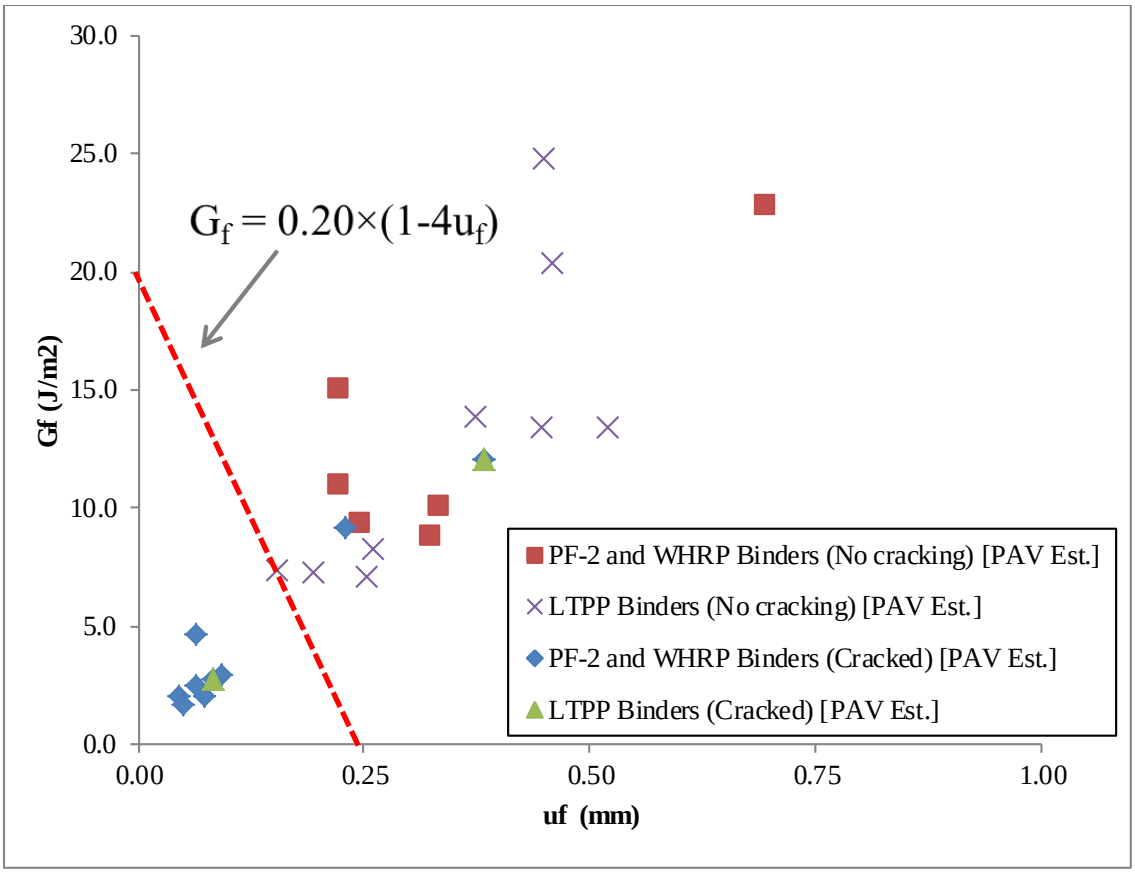

Figure 20. Example of estimated BBR-SENB specification graph at PAV-aged conditions (lower left triangle fails the specification)

Based on the results, it is suggested that the tests be conducted in PAV-aged condition and compared to the suggested limit line (applied to both RTFO and PAV-aged conditions), as the deteriorating effect of the PAV aging on BBR-SENB failure properties would make testing at this condition a more conservative methodology for controlling properties. A larger data set of PAV-aged binders corresponding to field performance will be needed to develop finalized limits to be potentially used in future WisDOT specification applications.

Proposed Procedure for Thermal Cracking Evaluation (BBR-SENB)

1. Prepare 3 BBR-SENB samples using the modified BBR molds (added notch) in accordance to AASHTO T 313 (BBR).
2. Condition samples for 1 hour at the required low temperature performance grade test temperature for the project location, in accordance to AASHTO M 320.
3. Perform load and displacement calibration similar to method described in AASHTO T 313 (BBR).
4. Load beam in displacement control mode at a rate of 0.01 mm/sec until failure occurs (total loading time is approximately 5 minutes).
5. Copy displacement, load, and calibration constants from output text file to analysis spreadsheet for automatic calculation of "G_f" and "u_f". Average the values over the results of the 3 replicates.
6. Compare the "G_f" vs. "u_f" result to the suggested preliminary failure criterion in Figure 18 for RTFO-aged binders. If G_f is smaller than $25\times(1 - 0.1\times u_f)$, fail the binder.

BBR-SENB Apparatus and Device Requirements

In order for the BBR-SENB device to be implemented as a specification test, some modifications to the standard Bending Beam Rheometer device are required. The following list outlines the main requirements and hardware modifications required:

Mold Assembly – The aluminum molds used in AASHTO T 313 should be modified to include notches on the side beam and a pin-hole assembly to keep the side beams and end pieces precisely aligned. This alignment is critical to insure proper notch location under the loading shaft. Figure 21 shows the modified mold assembly.

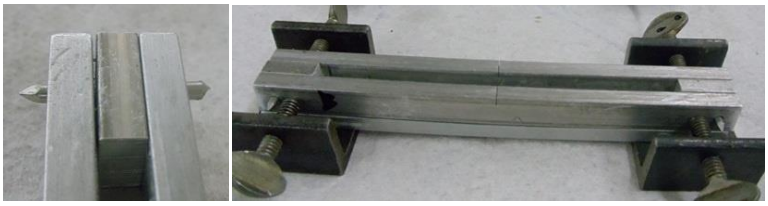

Figure 21. Modified mold assembly for preparation of BBR-SENB beams.

Loading Device – The Bending Beam Rheometer loading setup should be equipped with a step motor enabling the movement of the loading shaft at a constant and adjustable rate. The motor should be capable of applying rates of displacement between 0.0025 to 0.1 mm/sec. Figure 22 shows the motor setup and design.

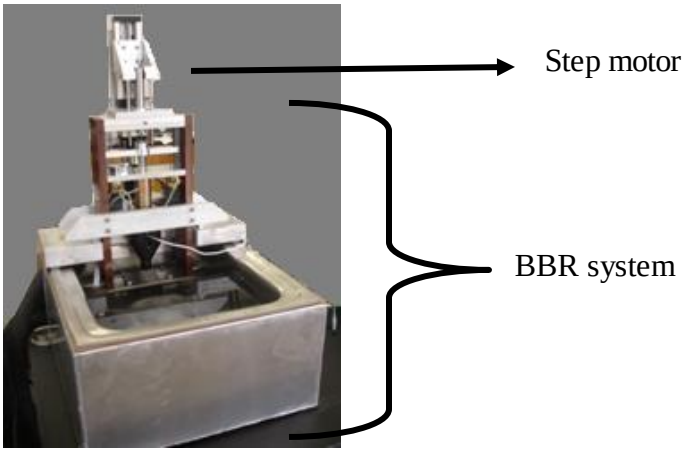

Figure 22. Loading device in BBR-SENB

Beam Supports – To ensure the proper alignment of the notch under the loading shaft, the beam support is modified to hold a beam with a width of 6.3 mm and an alignment bracket. Figure 23 shows the support and bracket design.

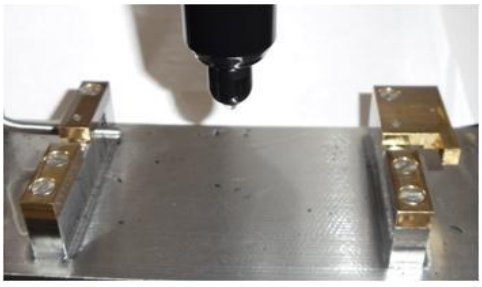

Figure 23. Beam supports to ensure notch alignment

Air Supply – The hose supplying pressurized air to the loading shaft air bearing should be equipped with a pressure regulator to allow adjusting air pressure between 138 Pa and 310 Pa.

Cooling Fluid – The Bending Beam Rheometer standardly uses Ethanol as the cooling fluid in the conditioning bath. A few of researchers have noted differences in strength values in the Direct Tension test (DTT) which have been attributed to the possibility of "Environmental Stress Cracking" caused by surface interactions between the sample and specific cooling fluids such as Ethanol (Marasteanu, et al., 2012). By request of the Binder Expert Task Group and as part of the Asphalt research Consortium study, the research team is investigating the need for use of alternative cooling fluids such as Potassium Acetate in the BBR-SENB system. Any future recommendations in this regard will be added to the draft AASHTO specification for the BBR-SENB test that is currently under consideration by the Binder ETG.

Summary and Conclusions for Thermal Cracking Evaluation of Binders

In this chapter the Single Edged Notched Beam procedure (BBR-SENB) was used for assessment of binder resistance to thermal cracking and results were compared to measured field performance. The following main conclusions were derived:

- Comparison of binders tested in both phase I and phase II showed that the critical cracking temperatures calculated using the BBR S(60) criterion or the DTT ultimate stress criterion seemed to roughly follow the same trend as the BBR-SENB G_f and u_f parameters, but with significantly less discrimination between the different binders.
- The BBR-SENB test was shown to be capable of clearly discriminating between modified and unmodified binders in a repeatable fashion.

- BBR-SENB results correlate well with the observed field thermal cracking PCI from the phase II condition survey, indicating the close relationship between this binder fracture test and the causal factors of thermal cracking in the field.
- A procedure and criteria is introduced for thermal cracking evaluation of modified binders using the BBR-SENB test at the project location low temperature PG specification temperature (average annual minimum pavement temperature + 10°C). The test method requires a modification to the current BBR setup for implementation, as was described in the chapter.
- Preliminary suggested failure limits and acceptance criterion were defined for qualifying binder results at RTFO-aged conditions in terms of thermal cracking resistance, showing the potential for this test to be eventually used as a specification test for modified and unmodified binders. Final failure criteria will require a larger data set at both RTFO and PAV-aged conditions to determine the most representative conditions for the procedure.

CHAPTER FOUR: RUTTING RESISTANCE

Background

The susceptibility of asphalt binders to rutting in the Superpave specification is determined based on limiting criteria on minimum binder stiffness and viscoelastic phase angle, through the evaluation of the binder's $|G^*|/\sin\delta$ parameter value, as defined by a Dynamic Shear Rheometer (DSR) at high performance temperatures. As this procedure assumes linear viscoelasticity in the test strain amplitudes, the inherent non-linearity of most modified binders is unaccounted for. During the NCHRP 9-10 project, Bahia et al. (2001) evaluated the direct correlation between mixture rutting properties and $G^*/\sin\delta$ on Rolling Thin Film Oven (RTFO) aged binders, tested at the same temperature at which the mixture Repeated Shear Constant Height (RSCH) tests were conducted. The results of this study and other research indicated a poor correlation between the mixture rate of accumulated strain and the parameter $G^*/\sin\delta$ measured at 10 rad/s (Bahia, et al., 2001b; Delgadillo, et al., 2006).

The repeated creep test was developed during the NCHRP 9-10 project to identify and isolate the viscous flow component contributing to the permanent deformation, from the total dissipated energy (D'Angelo, et al., 2006). The repeated creep and recovery test conducted using a DSR, measures the accumulated strain in the binder under a given stress level for a prescribed number of 1 second creep cycles followed by a 9 second recovery period. At least 100 cycles of loading was recommended. Tests were conducted at stress levels as low as 25 Pa and as high as 25.6 kPa (Delgadillo, et al., 2006). The irreversible loading in the RCR test makes it possible to differentiate between the permanent viscous strains that contribute to pavement rutting and delayed elastic strains that are recoverable. This is considered an advantage in comparison to the

cyclic reversible loading used for determination of the Superpave G*/sin δ parameter, for which separation of viscous and delayed elastic strain energy is not easily possible.

Since the introduction of the RCR, other studies have shown that creep and recovery under a single stress level does not allow for capturing possible non-linear viscoelastic behaviors of the binders, especially when polymer modified (D'Angelo, et al., 2007). Since running multiple tests at different stress levels using the 100 cycle RCR test requires an extensive amount of time, a shorter version of the test was introduced, later coming to be known as the Multiple Stress Creep and Recovery (MSCR) test (D'Angelo, et al., 2007).

The MSCR test, based on the RCR, was designed to reduce the number of tests and the number of repetitions needed at each stress level on a single sample for rutting characterization. In the development process the test used 10 cycles of 1-second creep loadings at 25, 50, 100, 200, 400, 800, 1600, 3200, 6400, 12800 and 25600 Pa stress levels, each followed by 9 seconds of recovery. The average non-recoverable strain at the end of each recovery step is averaged over the 10 cycles, normalized to the corresponding stress level, and referred to as the non-recoverable compliance (J_{nr}) (Bahia, et al., 2001). In the current standardized procedure, the test consists of 10 creep and recovery cycles at 0.1 kPa stress level, immediately followed by another 10 cycles of creep and recovery at a stress level of 3.2 kPa (D'Angelo, et al., 2007). The J_{nr} parameter has been suggested as a measure of the binder rutting behavior, and comparison of J_{nr} at the two stress level is suggested as a method to assess non-linearity of the binder response in this stress range, as described under AASHTO TP70 (AASHTO TP70, 2013).

Nonetheless, a number of concerns have been noted with regards to the current analysis protocols and testing conditions (Bahia, et al., 2011). This chapter uses the findings and discussions with regards to rutting mechanism from the previous chapters in combination with a

large number of experimental data from with the lab and from other labs across the country to address a number of these issues by suggesting simple revisions to the procedure conditions and setup.

Thus the main objective of this chapter is to evaluate the current MSCR procedure and propose revisions to the procedure where appropriate. The two main sources of concern with regards to the current standard MSCR test procedure are as follows:

1. *Adequacy of number of loading cycles*: In the NCHRP 9-10 project the need for a certain number of conditioning cycles before reaching a steady state response was first recognized for the binder creep and recovery test. The steady state response was defined as the state of consistent response with limited delayed elasticity effect carrying over from previous cycles (Bahia, et al., 2001).
2. *Adequacy of Stress Levels*: Asphalt binders at large strain levels often do not exhibit a linear viscoelastic response, therefore characterization of rutting behavior of asphalt based on low stress and strain measurements (e.g. Jnr at 0.1 kPa) will likely not accurately represent rutting resistance of asphalt mixture (Bahia, et al., 2011). Some researchers have shown that binder MSCR results at higher stress levels better correlate to mixture rutting performance (Dreessen, et al., 2009). The MSCR stress levels should be selected such as to reveal binder nonlinear behavior during rutting, and the number of cycles in each stress level should be adequate for achieving steady state response in the binder.

Results have shown that the standard 10 cycles per stress level are not sufficient to reach a stable steady state creep behavior, thus the addition of 20 conditioning cycles are recommended, for a total of 30 cycles for each stress level, the last 5 of which will be averaged

and reported for analysis. Furthermore, the current stress levels are deemed insufficient for accurate representation of binder stress state in the pavement, thus a higher stress level step (1o kPa) is recommended for addition to the test procedure. This modified method is currently being referred to as "MSCR Method B." The implications of these procedure modifications for current guidelines practice in Wisconsin will need to be carefully assessed.

Selected Projects

In phase I of the project although no section showed any sign of rutting, tests were performed on binders from field sections 9040-09-70, 9140-07-70, 7132-04-61, 1170-13-70, 1080-00-72. In the 2012 survey conducted as part of phase II no rutting was found in any of the surveyed sections either. The lack of any sign of rutting after 8-9 years of service indicate that rutting is not a critical issue of concern with modified binders. It is likely that meeting the required low temperature grade results in modification levels that exceed minimum requirements for rutting. This assumption is further investigated in this chapter.

Furthermore, due to the lack of any usable rutting performance data in the field sections it was decided to use binders from the MnROAD test track for which continuous rut depth monitoring data exists. The MnROAD test tracks located near Minneapolis experience similar climatic conditions as that of Wisconsin highways and were thus deemed an acceptable alternative for performance evaluation of modified binder high temperature characterization. The MnROAD cells were selected for this study are shown in Table 17.

Table 17. Selected MnROAD cells and binder modification properties

Name	Binder Grade	Modification Type
MnROAD 20	PG 58-28	Neat
MnROAD 22	PG 58-34	Elastomeric Modification
MnROAD 33	PG 58-34	PPA
MnROAD 34	PG 58-34	SBS+PPA
MnROAD 35	PG 58-34	SBS
MnROAD 77	PG 58-34	Elvaloy + Acid

Binder Testing

The binders from the Wisconsin field sections initially studied are shown in Table 18, along with the design ESALs and design traffic speed. This information was used to determine the AASTO MP 19 classification "grade" in terms of traffic and speed. As all sections had traffic volumes less than 10 million ESALs and design speeds higher that 70 km/h (43 mph), they were classified at the lowest grade, designated "S" in the MP 19 specification.

Table 18. Field sections tested at corresponding design ESALs and speed

Project ID	Design ESALs	Design Speed (mph)
9040-09-70	2,029,400	60
9140-07-70	1,511,101	55
7132-04-61	800,000	55
1170-13-70	2,284,900	45
1080-00-72	1,752,000	70

The binders were tested using the MSCR procedure, as shown in Figure 24. The tests were performed at RTFO conditions and at temperatures corresponding to the high temperature

performance of the corresponding field section's location. According to AASHTO MP 19, for an "S" grade binder the maximum allowable J_{nr} value is 4.0 kPa^{-1}. In comparison, the highest "grade" in AASHTO MP-19 ("E"), which pertains to slow moving traffic with volumes exceeding 30 million ESALs, the maximum allowable J_{nr} value is 0.5 kPa^{-1}. The maximum limit lines for the "S" and "E" grades are shown for comparison in Figure 24. It can be seen that all tested binders meet and exceed the requirements for both "S" and the "E" grades, showing that in accordance to AASHTO MP 19, the studied Wisconsin binders are extremely conservative in terms of rutting resistance. This is believed to also be the reason why no rutting damage was observed in any of the field surveys performed, even after 8-9 years in service.

Although tests were performed at three stress levels (100, 3200, 10,000 Pa), the ranking and relationships remained roughly the same, thus only the results at 3200 Pa are shown herein for the sake of brevity and for comparison to the AASHTO MP 19 specification values.

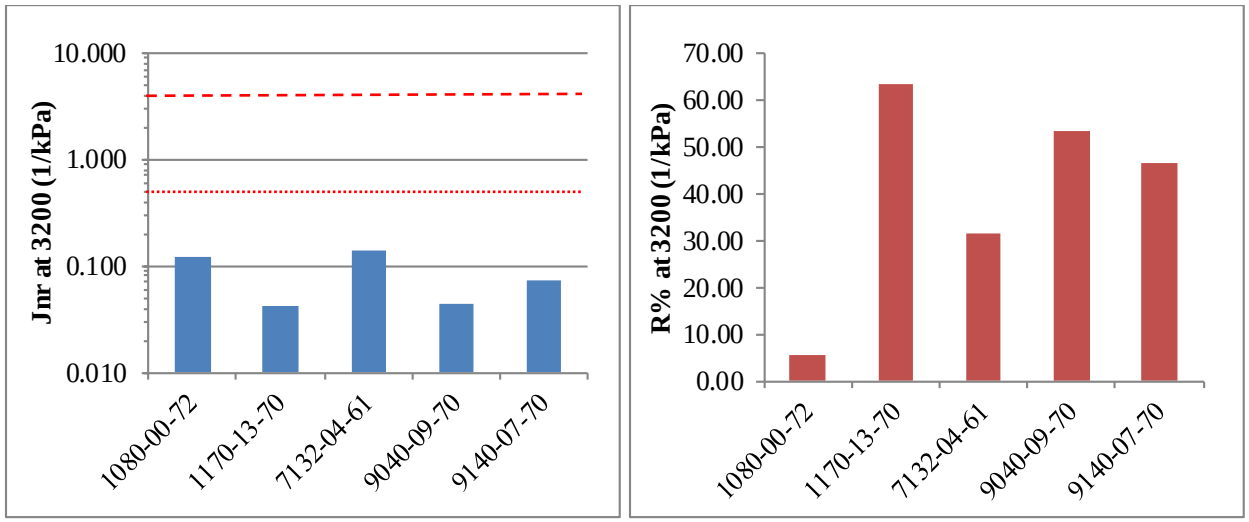

(a) **(b)**

Figure 24. Standard MSCR Results for binders at the local climate PG (dashed line shows AASHTO MP 19 limit for the "S" grade, dotted line shows the "E" grade limit)

As previously discussed, due to the lack of any visible rutting in the Wisconsin sections, a number of MnROAD binders were selected for evaluation of the rutting binder criteria. The binders selected were tested at RTFO conditions using the Superpave procedure to determine the variation of |G*|/sinδ with temperature, as shown in Figure 25. Based on the results, binders C-20 and C-22 should be categorized as PG 64, while binders C-33, C-34, and C-77 will be designated as PG 70. Binders C-22 and C-33 barely missed the threshold values for PG 70 and PG 76, respectively.

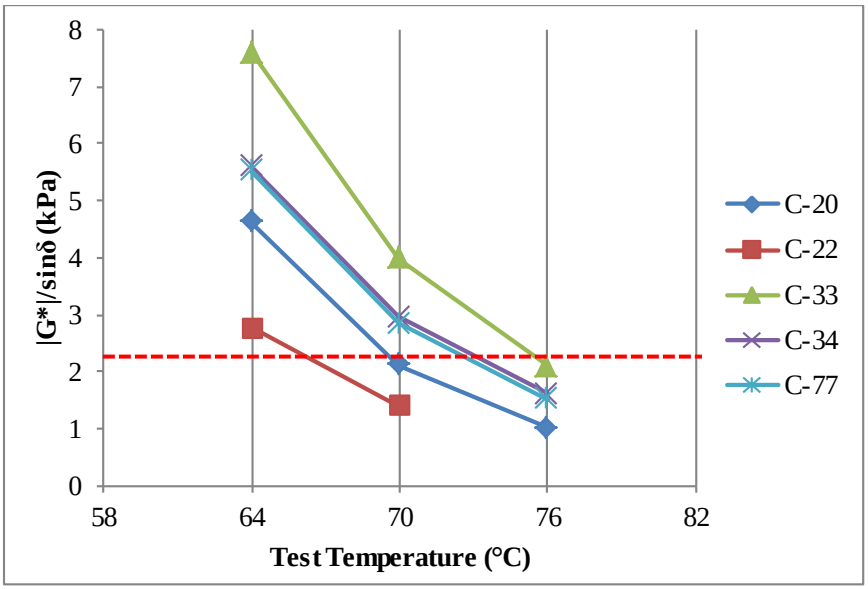

Figure 25. Superpave rutting test results at multiple temperatures (dashed line is RTFO grade criteria)

The MSCR test was performed on the MnROAD binders following both the standard method (AASHTO TP 70) and the proposed modified method using the average of the last 5 of 30 cycles per stress level (method B). The results are shown for both Jnr and the percent of recovery in Figure 26. A difference is observed between the standard and the method B MSCR tests. Although the difference is not very large in magnitude for the binders tested, it consistently shows a poorer performance for the binders (i.e. higher Jnr and lower percent recovery). This indicates that for the binders tested in the standard method for which the average of all cycles are

considered the results are less conservative than that of method B in which 25 cycles of conditioning is used at each stress level to achieve a steady state response from the binder, before average the results of the next 5 cycles.

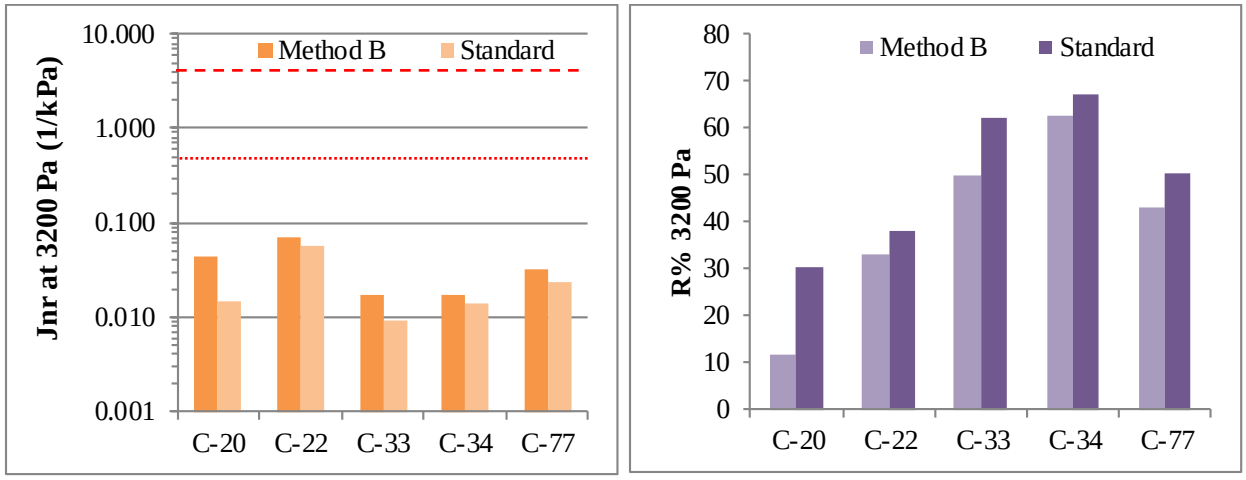

(a) **(b)**

Figure 26. MSCR Results for MnROAD binders at 58°C (dashed line shows AASHTO MP 19 limit for the "S" grade, dotted line shows the "E" grade limit)

In the next step the MSCR test results were compared to the field performance data from the MnROAD test track. The data was acquired from the MnROAD database. Rut depth was measured using an Automated Laser Profile System (ALPS), which measures transverse surface profile at 0.25 inch intervals with a laser. Measurements were made every 2-3 months through 2011. To insure similar number of traffic loading over all sections, the rut depth after 30 months of loading was derived for all sections using a linear fit to the gathered data. The results are shown in Table 19.

Table 19. Rutting Performance of MnROAD cells after 30 months of loading

MnROAD Cell	Rut Depth (in)	Rut Rate (in/month)
C-20	0.11	0.0026
C-22	0.14	0.0031
C-33	0.12	0.0025
C-34	0.21	0.0054
C-77	0.15	0.0025

Figure 27 shows a comparison of the field rutting performance and that of the binders under both MSCR test methods. No relation is seen between either the $G^*|/\sin\delta$ parameter or the MSCR J_{nr} results with the observed rut depth, although a slight improvement was seen when using the Method B (average of last 5 of 30 cycles). The results highlight an important aspect of rutting damage, which is the important contribution of factors other than the binder, such as aggregate structure, to resistance against rutting.

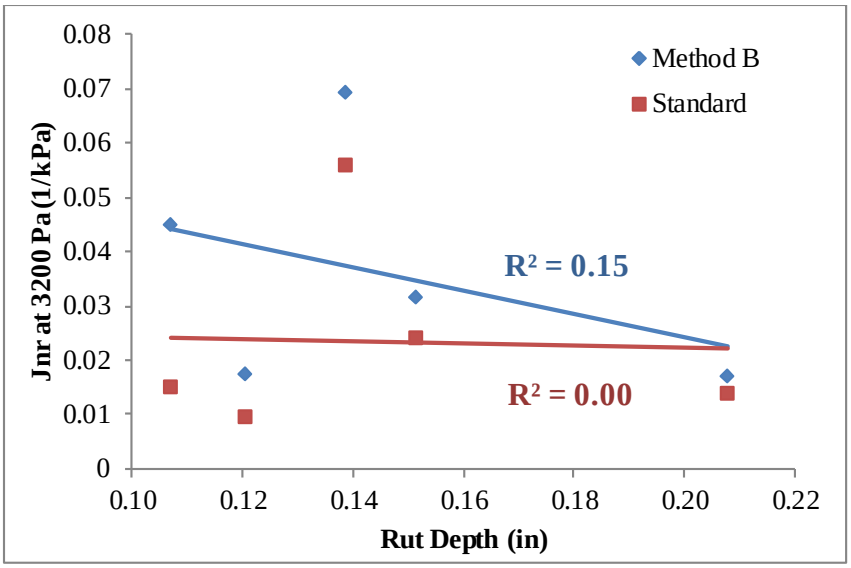

(a)

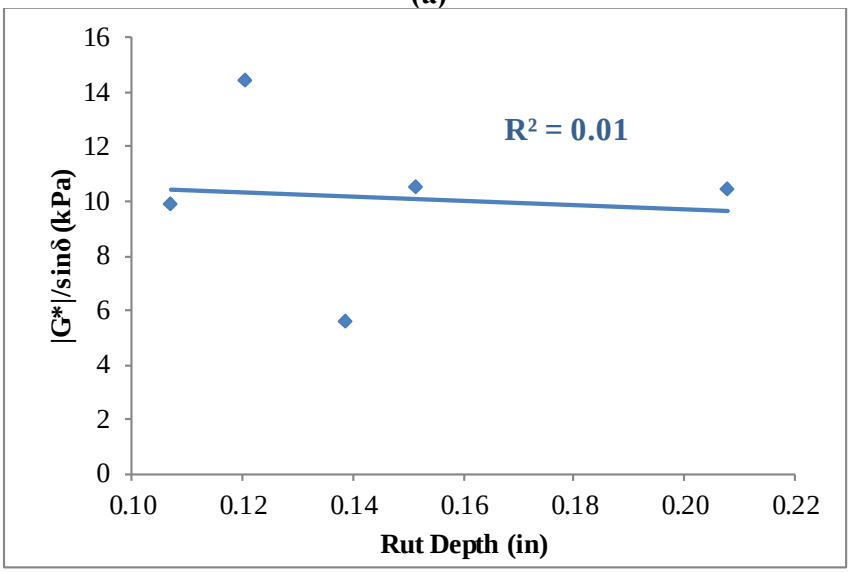

(b)

Figure 27. Comparison of binder measures (G*|/sinδ and J_{nr}) and the observed field rut depth

MnROAD sections C-33, C-34, and C-77 were originally constructed as part of a study on the effects of PPA modification, as part of which rutting characterization of the binder and mixture was performed using laboratory constructed and field-extracted samples (Reinke, 2008). The study showed that short term aging during construction varied for the different binders, resulting in field recovered binders that were significantly more aged in the field compared to the RTFO aging level for sections C-33 and C-34, while less aging had occurred in the field for

section C-77 compared to that of RTFO-aging. Although it is expected that higher aging would improve rutting resistance, the pavements in sections C-33 and C-34 rutted more than the lesser-aged C-77 pavement. These results highlight the importance of construction conditions, especially short term aging, for rutting characteristics of binder, while further complicating establishment of a direct relationship between the binder properties and resultant field rutting. Reinke (2008) also noted that an opposite trend was observed between laboratory RTFO-aged MSCR results and mixture wheel-tracking rut depth. While using binder recovered from the field corrected the trend, in was noted by Reinke (2008) that the MNROAD field sections rutted more than would be expected based on the binder rheology and MSCR results and tentatively attributed this to the possible effect of aggregate absorption levels on the effective binder content in these mixtures. These finding are in-line with observations in the present study, prompting the investigation of the mixture aggregate structure and its relation to the observed rutting performance, as is discussed in the next section.

Characterization of internal aggregate structure by means of Digital Imaging Analysis

The heterogeneous multiphase components of asphalt concrete, consisting of aggregates, asphalt binder, and air voids, constitute a complex microstructure. Based on the contact mechanism analysis, Zhu and Nodes (2000) demonstrated that the transmission of load in the asphalt mixture is mainly determined by the interaction of aggregates and binder at the contacts of adjacent aggregates. Changes in mechanical and geometrical parameters in aggregate and binder will affect the overall stress-strain distribution in an asphalt mixture. The contact based stress-strain equations and models for asphalt mixtures show that the geometrical properties of the aggregate proximity zone such as proximity area, number of proximity zones and proximity orientation

affect the stress distribution in the mixture as a whole (Zhu & Dass, 1996; Zhu, 1998). It has been demonstrated that the directional distribution of the asphalt mixture micromechanical properties affect its response to loading (Tashman et al., 2004; Wang et al., 2004). Additionally, it has been shown that the aggregate gradation affects the internal structure and the stress distribution in asphalt mixtures (Masad, et al., 1999).

Image processing and quantification of the internal structure features in the current study were conducted using a 2-D image processing software named "IPAS 2". The details of the image processing procedure are explained in publications by Coenen et al. (2011) and Roohi et al. (2012). The volumetric properties and gradation of the mixture were entered as an input to the software to calculate the volume fraction of aggregates in mix as an accuracy control of area fraction of aggregates captured in the image. Based on processed image, the software performs a virtual sieve analysis. Users can control the quality of aggregate structure captured based on comparisons of the real and virtual gradation of the mixture and the volume (real) and area (virtual) fraction of aggregates in mixture.

To obtain usable images, the samples (cores or SGC samples) are cut in three sections leading to attainment of six 2-D images, with one cutting section at the middle of the sample and two in the one inch distance from the middle section (producing 4 slices of equal volumes). The surface of face of each cur is scanned using a flatbed scanner and entered into the IPAS2 software.

In the software, proximity is defined when two aggregates' perimeter pixels are within a distance specified by the user and all the pixels of the two aggregates' perimeter within this distance are captured. These pixels form the contact lines. For each pixel of the aggregate number one there is one and only one pixel on the perimeter of the aggregate number two with a

distance less than the predefined value (if there are several, the closest pixel). This procedure is depicted in Figure 28.

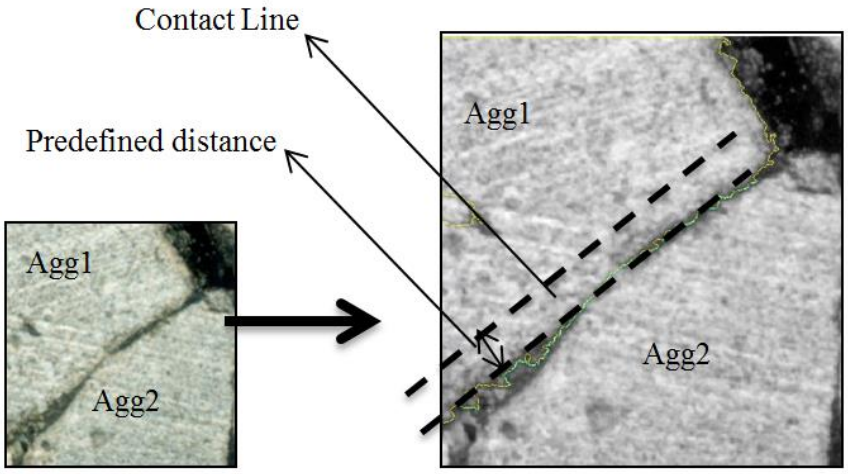

Figure 28. Illustration. Definition of the aggregate proximity line

Thereafter, the calculation of the normal to contact orientation (angle from horizontal axis) can be performed. The implemented procedure connects the contact pixels using straight lines and calculates the slope perpendicular to these straight lines. Thereafter, the vector that represent these directions is determined, which defines the normal to contact orientation. Figure 29 shows the procedure schematically.

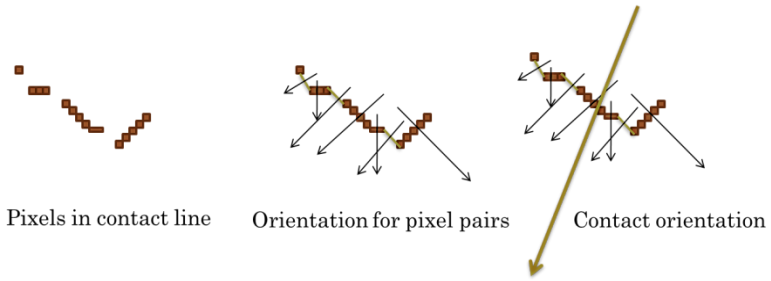

Figure 29. Illustration. Schematic of contact orientation calculation

Contact length and orientation are both important parameters to characterize the internal structure of mixture. Differences in contact areas (length) produce different stress intensities and aggregate interlocking, consequently affecting performance. In addition, the contact orientations define the effectiveness of contacts in carrying the load. The closer the direction of the normal to contact orientation to that of axial loading (i.e., 90 degrees in this case), the more effective the contact is in resisting the axial load. Figure 30 shows contact lines and orientation for a mix under axial loading.

As previously discussed, aggregate skeleton is the structure of aggregates that are connected in the loading direction (from top to bottom of the sample in this case). In order to measure the internal structure indices of the skeleton, aggregates that are not in the skeleton were neglected (i.e. single or single contacted aggregates, set of aggregates that are not connected to the aggregates in top and bottom of the mixture). Figure 31 shows a black and white image of a mix and the skeleton of aggregates represented in contour image and lines that link the contact zones of aggregates.

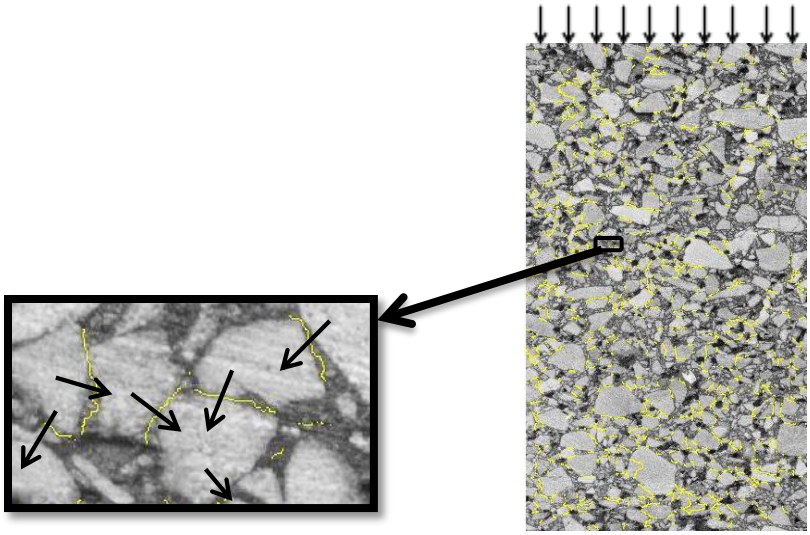

Figure 30. Illustration. Contact lines and orientation in real mixtures. (Normal to contacts lines are shown with arrows).

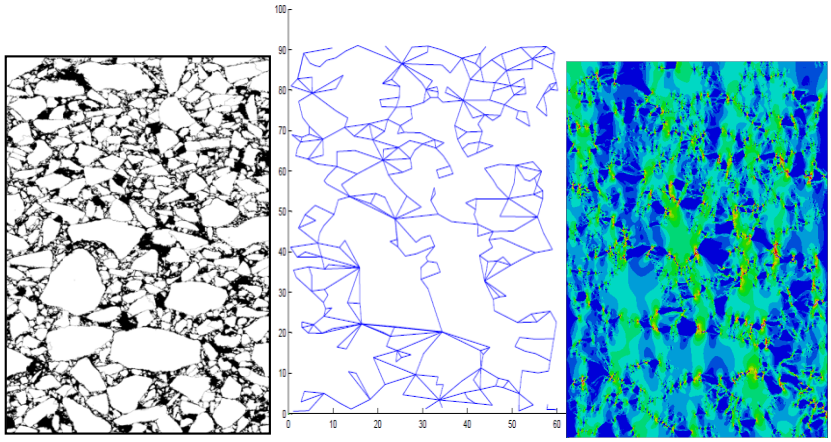

Figure 31. Illustration. Aggregate skeleton- connectivity (lines represent stress paths)

Thus based on the previous studies, the Total Proximity Length (TPL), which is directly derived as output from the IPAS2 image analysis, has been proposed as a representative measure of the internal structure quality and a necessary complement to assessment of rutting resistance based on the binder phase. Mixtures with higher TPL will accumulate less permanent deformation under repeated creep.

Performance Data

The aggregate structure of the MnROAD mixtures were assessed using the method described in the previous section. To this end the gradations were determined, as shown in Figure 32. It is seen that C-20 has the finest gradation, followed by C-22. These sections also showed better rut resistance compared to the other studied sections. The reason for this was shown by analyzing the scanned images of the cut surfaces of the mixtures using IPAS2, examples of which are shown in Figure 33.

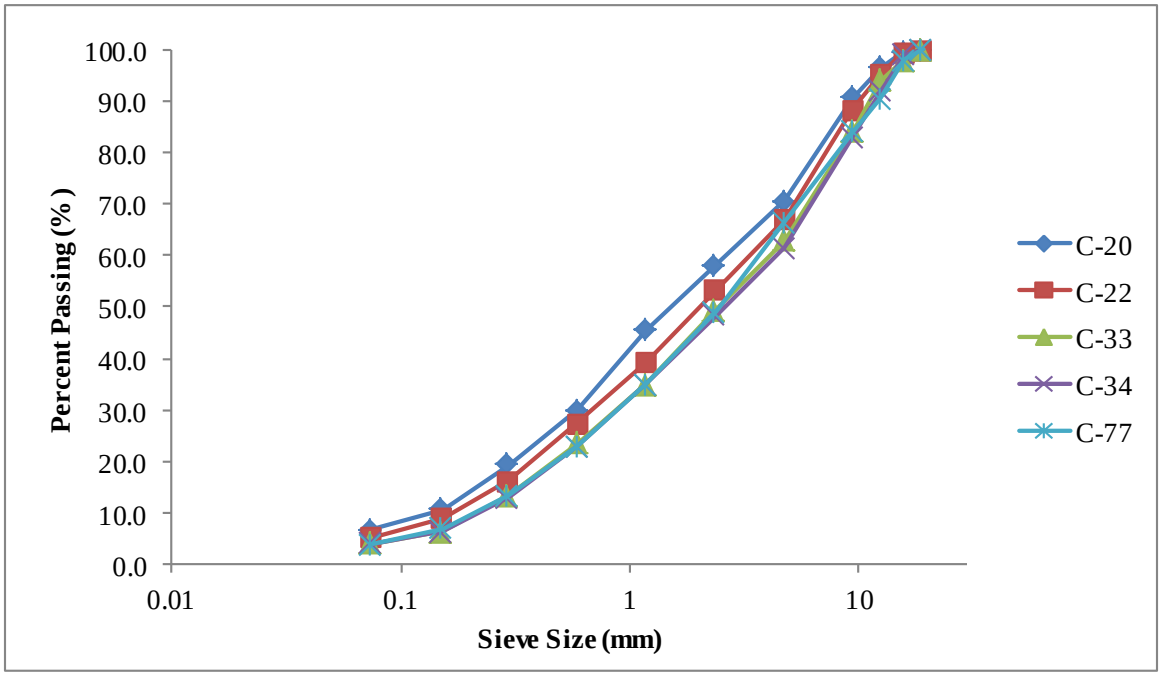

Figure 32. Gradation of MnROAD test sections

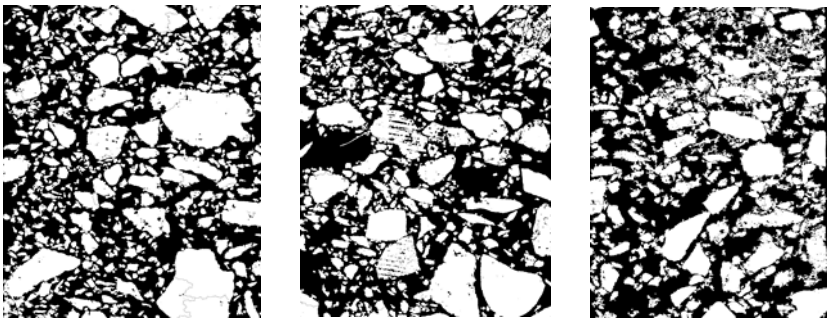

(a) **(b)** **(c)**

Figure 33. Filtered images of aggregate structure for (a) C-77, (b) C-22, and (c) C-20.

The results of the aggregate structural analysis using the total proximity length (TPL) parameter is shown in Figure 34 for the four sections from which mixture samples and images was available. It is immediately apparent that a relationship exists between higher TPL and lower rut depth. A higher TPL would indicate a better aggregate load transfer, as the total aggregate area in contact throughout the effective load-bearing aggregate structure is higher than that of mixtures with lower TPL. The results indicate the importance of assessing both the aggregate properties and the binder performance for analysis of rutting resistance in paving material. This becomes even more essential when considering recent findings showing that use of different modifiers can lead to significantly different TPL in the mixture using identical gradations (Teymourpour, et al., 2013).

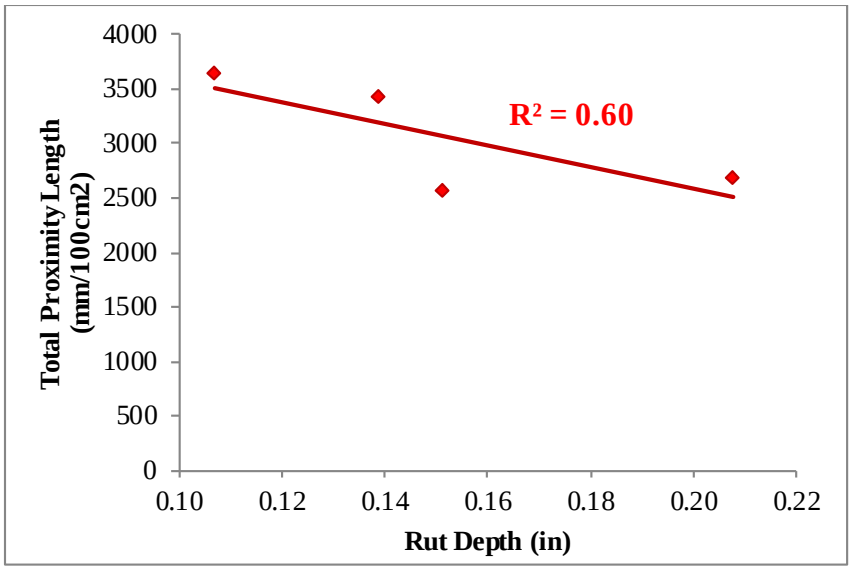

Figure 34. Comparison of TPL and field performance (rut depth)

Finally a regression analysis was performed between the observed rut depth, the aggregate structure (TPL), and binder properties (J_{nr} at 3.2 kPa from both MSCR methods and the PG G*/sinδ). The results are shown in Table 20, in which it is seen that in 1 of the 3 scenarios the binder coefficient is in the opposite direction of that intended. Although it is understood that statistical analysis based on such limited number of data points is inconclusive, the mixed results seem to indicate that both the binder properties and the aggregate structure are necessary from proper analysis of pavement rutting resistance, such that with a good aggregate structure the pavements with the poorest binders (the unmodified C-20) was able to perform better than the other modified and high performing binders in terms of rutting resistance. Thus based on the results of the studied binders and the corresponding field performance, no recommendation can be made at this point with regards to selection of a binder rutting resistance test and parameter.

Table 20. Regression analysis results for binder and aggregate rutting paramters against a rut depth response

Response: Rut Depth (in)	Coefficient	P-value	R^2
Constant	0.3918	0.371	62.1%
G*/sinδ (kPa)	-0.00335	0.838	
TPL	-0.00006833	0.443	

Response: Rut Depth (in)	Coefficient	P-value	R^2
Constant	0.3374	0.274	59.6%
Jnr 3.2kPa (Standard)	0.44	0.981	
TPL	-0.00006089	0.453	

Response: Rut Depth (in)	Coefficient	P-value	R^2
Constant	0.3146	0.326	61.8%
Jnr 3.2kPa (Method B)	-0.421	0.85	
TPL	-0.00004753	0.629	

Summary and Conclusions for Evaluation of Rutting Resistance

In the present chapter it was shown that the studied Wisconsin binders exceeded the most extreme binder rutting grade requirements according to AASHTO MP 19 (MSCR) at the local high performance temperatures. The results confirm previous notions that rutting is not a significant concern in Wisconsin and development of an advanced binder criteria and classification systems for rutting resistance of binders may not be as essential as that of thermal and fatigue cracking. The following main conclusions were derived:

- Binder rutting parameters (|G*|/sinδ and the standard and modified procedure (method B) MSCR) were unable to relate directly to the observed field conditions for studied sections. For the tested binder set, the unmodified binder showing the worse performance in terms of both |G*|/sinδ and MSCR, performed better in the field in terms of accumulated rut depth.

- It was shown that the aggregate structural was able to capture a trend that better reflected that of the field rutting behavior.
- Results indicate that there no rutting is observed in any section in Wisconsin. In addition looking at MnROAD sections there is some indications of rutting (0.1 to 0.2 in) that could not be explained solely through use of binder properties. Both $|G^*|/\sin\delta$ and Jnr were used in the analysis, but it appears that a consideration of aggregate structure is needed to relate to this minor variation in rutting. Therefore at this time it is difficult to recommend any changes in binder rutting parameters based on the current set of data.

CHAPTER FIVE: CONCLUSIONS AND RECOMMENDATIONS

In the present study a set of modified binders corresponding to constructed field section across Wisconsin were tested using recently developed characterization procedures under consideration or standardized by AASHTO as provisional standards. The purpose of the project was to identify promising procedures and applicable modified binder specification criteria for use in Wisconsin, based on comparison of test results to field performance. Field performance was assessed through condition surveys conducted between 2004 and 2012 as part of both phase I and phase II of the project. The following main conclusions and findings were made:

Fatigue Characterization

The Linear Amplitude Sweep test, standardized under AASHTO TP101, was considered and evaluated and the resulting Nf value was investigated as a potential parameter for ranking binders in terms of expected resistance to fatigue cracking. The following main findings were discussed:

- The Superpave $|G^*|\sin\delta$ parameter was found to relate poorly to the field performance of the modified binders investigated in the current study. The parameter also did relate to Np20 or the LAS Nf parameter.
- Two failure criteria were evaluated for calculation of the "A" parameter in the LAS fatigue power law. It was shown that both criteria resulted in correct trends and fair to very good correlations with field performance. The best correlations were found using the Nf corresponding to the damage level at the peak stress.

- It is recommended as a future activity that the use of |G*|sinδ results for derivation of the LAS "B" parameter be investigated. This would allow for conducting the LAS test on the same sample as the PG test by simply adding a strain sweep step after the conclusion of the |G*|sinδ loading cycles.
- Based on the results of phase I and phase II analyses, the Linear Amplitude Sweep test performed at the required Superpave intermediate temperature grade of the project location, and the resultant N_f at peak stress parameter, are recommended for use for evaluation of modified binder fatigue damage resistance.
- A test procedure as well as preliminary N_f minimum allowable limits and criterion were based on RTFO-aged conditions were suggested based on comparison to field performance Development of final acceptance limits will require data from a larger set of binders at both RTFO and PAV-aged conditions to select the most suitable condition for possible use in future specification.
- In the present study the fresh binder retained from these projects during construction was laboratory aged and used for comparison to field performance, while the complexity of the possible effect of RAP binder replacement was avoided. Future studies may benefit from binder extraction from the monitored pavement sections to better assess possible effects of RAP binder replacement as well as direct field aging on binder performance and relevance to laboratory aged properties and characterization procedures.

Low Temperature Characterization

The Single Edged notched Bending procedure (BBR-SENB), based on the modification of the Bending Beam Rheometer test was used to assess the Wisconsin modified binders in terms of

resistance to thermal cracking. This procedure is currently under consideration by AASHTO for provisional standardization. The following main conclusions were derived:

- Comparison of binders tested in both phase I and phase II showed that the critical cracking temperatures calculated suing the BBR S(60) criterion or the DTT ultimate stress criterion seemed to roughly follow the same trend as the BBR-SENB G_f and u_f results, but with significantly less discrimination between the different binders.
- The BBR-SENB test was shown to be capable of clearly discriminating between modified and unmodified binders in a repeatable fashion.
- BBR-SENB results correlate well with the observed field thermal cracking PCI from the phase II condition survey, indicating the high promise of using this binder fracture test as modified and unmodified binder low temperature characterization test to complement the current BBR test.
- A procedure was introduced for thermal cracking evaluation of modified binders using the BBR-SENB test at the project location low temperature PG specification temperature (average annual minimum pavement temperature + 10°C). A preliminary failure limit and acceptance criterion was defined for qualifying binder results in terms of thermal cracking resistance using RTFO aged binders and estimated for PAV-aged conditions. Based on the current data it is recommended that PAV-aged conditions be used for a more conservative controlling of binder failure properties. Development of final acceptance limits will require data from a larger set of binders at both RTFO and PAV-aged conditions to select the most suitable condition for possible use in future specification.

Rutting Characterization

It was shown that the studied Wisconsin binders exceeded the most extreme binder rutting grade requirements according to AASHTO MP 19 (MSCR) at the local high performance temperatures. The results confirm previous notions that rutting is not a significant concern in Wisconsin and development of advanced binder criteria and classification systems for rutting resistance of binders may not be as essential as that of thermal and fatigue cracking. The following main conclusions were derived:

- Binder rutting parameters ($|G^*|/\sin\delta$ and the standard and modified procedure (method B) MSCR) were unable to relate directly to the observed field conditions for studied sections. For the tested binder set, the unmodified binder showing the worse performance in terms of both $|G^*|/\sin\delta$ and MSCR, performed better in the field in terms of accumulated rut depth.
- It was shown that the aggregate structural was able to capture a trend that better reflected that of the field rutting behavior.
- Results indicate that there no rutting is observed in any section in Wisconsin. In addition looking at MnROAD sections there is some indications of rutting (0.1 to 0.2 in) that could not be explained solely through use of binder properties. Both $|G^*|/\sin\delta$ and Jnr were used in the analysis, but it appears that a consideration of aggregate structure is needed to relate to this minor variation in rutting. Therefore at this time it is difficult to recommend any changes in binder rutting parameters based on the current set of data.

REFERENCES

AASHTO TP70, 2013. *Standard Method of Test for Multiple Stress Creep Recovery (MSCR) Test of Asphalt Binder Using a Dynamic Shear Rheometer (DSR),* Washington, D.C.: American Association of State Highway and Transportation Officials.

Bahia, H. et al., 2001. *Characterization of Modified Asphalt Binders in Superpave Mix Design,* Washington, D.C.: National Academy Press.

Bahia, H., Tabatabaee, H. & Velasquez, R., 2012. *Importance of Bitumen Physical Hardening for Thermal Stress Buildup and Relaxation in Asphalt.* Istanbul, Turkey, s.n.

Bahia, H., Tabatabaee, N., Clopotel, C. & Golalipour, A., 2011. *Evaluation of the MSCR Test for Modified Binder Specification.* s.l., s.n.

Bahia, H. U. et al., 2001. *Characterization of Modified Asphalt Binders in Superpave Mix Design, NCHRP Report 459,* Washington, D.C.: National Academy Press.

Bahia, H., Velasquez, R., Tabatabaee, H. & Puchalski, S., 2012. *The Role of Asphalt Binder Fracture Properties in Thermal Cracking Performance of Mixtures and Pavements.* s.l., s.n.

Bahia, H. et al., 2001b. Development of binder specification parameters based on characterization of damage behavior. *Asphalt Paving Technology,* pp. 442-470.

Chailleux, E. & Mouillet, V., 2006. *Determination of the low temperature bitumen cracking properties: fracture mechanics principle applied to a three points bending test using a non-homogeneous geometry.* Quebec, s.n.

Clopotel, C. & Bahia, H., 2012. Importance of Elastic Recovery in the DSR for Binders and Mastics. *Engineering Journal,* 16(4).

Coenen, A., M.E., K. & H.U., B., 2011. Aggregate Structure Characterization of Asphalt Mixtures Using 2-Dimensional Image Analysis. *International Journal of Road Materials and Pavement Design.*

D'Angelo, J., Dongre, R. & Reinke, G., 2006. *Evaluation of Repeated Creep and Recovery Test Method as an Alternative to SHRP+ Requirements for Polymer Modified Asphalt Binders.* s.l., s.n.

D'Angelo, J., Dongre, R. & Reinke, G., 2007. Creep and Recovery. *Public Roads,* 70(5), pp. 24-30.

D'Angelo, J. K. R., Dongre, R., Stephens, K. & Zanzotto, L., 2007. Revision of the Superpave High Temperature Binder Specification: The Multiple Stress Creep Recovery Test. *Asphalt Paving Technology,* 76(123).

Delgadillo, R. & Bahia, H., 2005. Rational Fatigue Limits For Asphalt Binders Derived From Pavement Analysis. *Journal of the Association of Asphalt Paving Technologists,* Volume 74.

Delgadillo, R., D.W., C. & H.U., B., 2006. Nonlinearity of Repeated Creep and Recovery Binder Test and Relationship with Mixture Permanent Deformation. *Transportation Research Records: Journal of the Transportation Research Board,* Volume 1962.

Delgadillo, R., Nam, K. & H.U., B., 2006. Why do we need to change G*/sin δ and How?. *Road Materials and Pavement Design,* Volume 7.

Dongré, R. & D'Angelo, J., 1998. *Effect of New Direct Tension Test Protocol on the Superpave Low-Temperature Specification for Bitumen Binders.* s.l., s.n.

Dreessen, A., Planche, J. & Gandel, V., 2009. *A new performance related test method for rutting prediction: MSCRT.* s.l., s.n.

Hesp, S., 2003. *An improved low-temperature asphalt binder specification method,* s.l.: NCHRP-IDEA contract 84 and Ministry of Transportation Ontario Contract 9015-A-000190.

Hintz, C., 2012. *Understanding Mechanisms Leading to Asphalt Binder Fatigue,* s.l.: University of Wisconsin-Madison.

Hintz, C., Velasquez, R., C., J. & Bahia, H., 2011. Modification and Validation of the Linear Amplitude Sweep Test for Binder Fatigue Specification. *Transportation Research Record: Journal of the Transportation Research Board.*.

Hoare, T. & Hesp, S., 2000. Low-Temperature Fracture Testing of Asphalt Binders: Regular and Modified Systems. *Transportation Research Record: Journal of the Transportation Research Board,* Volume 1728.

Johnson, C. & Bahia, H., 2010. Evaluation of an Accelerated Procedure for Fatigue Characterization of Asphalt Binders. *Submitted for publication in Road Materials and Pavement Design.*

Kose, S., Guler, M., Bahia, H. U. & Masad, E., 2000. Distribution of strains within asphalt binders in HMA Using Image and finite element techniques. *Trans Res Record National Research Council.*

Marasteanu, M. et al., 2012. *Investigation of Low Temperature Cracking in Asphalt Pavements, National Pooled Fund Study -Phase II,* St. Paul, MN: Minnesota Department of Transportation.

Marasteanu, M., Cannone Falchetto, A., Turos, M. & Le, J.-L., 2012. *Development of a Simple Test to Determine the Low Temperature Strength of Asphalt Mixtures and Binders,* Washington D.C.: Transportation Research Board of the National Academies.

Masad, E., Muhunthan, B., Shashidhar, N. & Harman, T., 1999. Internal Structure Characterization of Asphalt Concrete Using Image Analysis. *Journal of Computing in Civil Engineering (Special Issue on Image Processing),* 13(2), pp. 88-95.

Nam, K., Delgadillo, R. & Bahia, H., 2005. *Development of Guidelines for PG Kitae Nam, Rodrigo Delgadillo and Hussain Bahia.,* Madison: Wisconsin Highway Research Program.

Reinke, G., 2008. *Report tp Innophose on PPA Modified Binder Mixes Placed at MnROAD Test Site in Summer of 2007*, Onalaska, WI: Mathy Technology & Engineering Services, Inc.

Roohi, N., Tashman, L. & Bahia, H., 2012. Internal Structure Characterization of Asphalt Mixtures for Rutting Performance Using Imaging Analysis. *Journal of Road Materials and Pavement Design,* Volume 13, pp. 21-37.

Roohi, N., Teymourpour, P. & Bahia, H., 2013. Effect of Particle Mobility on Aggregate Structure Formation in Asphalt Mixtures. *Journal of the Association of Asphalt Paving Technologists.*

Safaei, F. et al., 2013. Implications of Warm-Mix Asphalt on Long Term Oxidative Aging and Fatigue Performance of Asphalt Binders and Mixtures. *Submitted to the Journal of the Association of Asphalt Pavement Technologists.*

Teymourpour, P., Hacker, S. & Bahia, H., 2013. *Role of Asphalt Modification in Achieving Better Aggregate Packing Structure and Performance.* s.l., s.n.

Velasquez, R., Tabatabaee, H. & Bahia, H., 2011. Low Temperature Cracking Characterization of Asphalt Binders by Means of the Single-Edge Notch Bending (SENB) Test. *Journal of the Association of Asphalt Pavement Technologists.*

Zhu, H., 1998. *Contact Mechanism Based Asphalt Concrete Modeling*. San Diego, California, s.n.

Zhu, H. & Dass, W., 1996. *Modeling of asphalt concrete: Technical Report on the project of Asphalt Concrete Constitutive Behavior to WL/FIVC,* Florida: Applied Research Associates, Inc..

Zhu, H. & Nodes, J., 2000. Contact based analysis of asphalt pavement with the effect of aggregate angularity. *Mechanics of Materials,* Volume 32, pp. 193-202.

Wisconsin Highway Research Program
University of Wisconsin – Madison
1415 Engineering Drive
Madison, WI 53706
http://wisdotresearch.wi.gov/whrp